Aquaculture 591 (2024) 741137

Contents lists available at ScienceDirect

Aquaculture

journal homepage: www.elsevier.com/locate/aquaculture

# A novel antimicrobial peptide Spasin$_{141\text{-}165}$ identified from *Scylla paramamosain* exhibiting protection against *Aeromonas hydrophila* infection

Chang Zhang [a,b], Fangyi Chen [a,b,c,*], Yuqi Bai [a,b], Xianxian Dong [a,b], Xinzhan Meng [a,b], Ke-Jian Wang [a,b,c,*]

[a] State Key Laboratory of Marine Environmental Science, College of Ocean & Earth Sciences, Xiamen University, Xiamen, Fujian, China
[b] State-Province Joint Engineering Laboratory of Marine Bioproducts and Technology, College of Ocean & Earth Sciences, Xiamen University, Xiamen, Fujian, China
[c] Fujian Innovation Research Institute for Marine Biological Antimicrobial Peptide Industrial Technology, College of Ocean & Earth Sciences, Xiamen University, Xiamen, Fujian, China

ARTICLE INFO

*Keywords:*
Antimicrobial peptide
Spasin$_{141\text{–}165}$
Antimicrobial activity
*Scylla paramamosain*
*Aeromonas hydrophila* infection

ABSTRACT

*Aeromonas hydrophila* is a widely distributed Gram-negative waterborne pathogen responsible for large-scale outbreaks of hemorrhagic septicemia in fish, causing severe economic losses to the global aquaculture industry. In view of few therapeutic drugs currently available for use in aquaculture and the emergence of multidrug-resistant *A. hydrophila*, there is an urgent need to develop new antimicrobial agents as an alternative to antibiotics. Antimicrobial peptides (AMPs) have strong antimicrobial effects and unique machanisms of action, and are not easy to induce bacterial resistance, making them an ideal alternative to antibiotics. In this study, we identified a new functional gene from marine crab *Scylla paramamosain*, named Spasin, which encodes a mature peptide of 240 amino acids and expressed widely in various tissues of crabs. Notably, a truncated peptide Spasin$_{141\text{–}165}$ derived from Spasin, showed potent and broad-spectrum antibacterial and antifungal activity at minimum inhibitory concentrations (MICs) ranged from 0.75 μM–48 μM, which is a novel AMP. It effectively killed *S. aureus* and *A. baumannii* within 2 h and 90 min, respectively. Importantly, it is not toxic to HEK-293 T, RAW 264.7, and ZF4 cell lines. Mechanistic studies showed that addition of 8 μg mL$^{-1}$ lipoteichoic acid or lipopolysaccharides decreased bacterial susceptibility to Spasin$_{141\text{–}165}$. In addition, Spasin$_{141\text{–}165}$ altered the permeability of the inner and outer cell membranes, and resulted in the release of ATP and the accumulation of intracellular reactive oxygen species. Notably, Spasin$_{141\text{–}165}$ significantly increased the survival rate of zebrafish infected with *A. hydrophila*, redcued the bacterial load in the spleen, and effectively inhibited the expression of inflammation-associated factors (*e.g.*, IL-1β, TNF-α, *etc.*). Taken together, Spasin$_{141\text{–}165}$ is a potential antibacterial agent for the treatment of *A. hydrophila* infections in aquaculture and a promising antibiotic alternative.

## 1. Introduction

Microbial infections pose a major threat to fisheries and livestock production, as well as to human health (Browne et al., 2021). Antibiotics have greatly contributed to the development of fisheries and livestock since their discovery. For example, antibiotics are widely used to combat diseases caused by microbial pathogens. Unfortunately, the misuse of antibiotics has led to a serious problem of microbial resistance, which, in turn has resulted in treatment failures, increased morbidity and mortality, and higher medical expenses (Ding et al., 2023). Antibiotics have been widely used in livestock to improve growth and productivity, and their use is gradually increasing. Use of antibiotics in non-human animals may also lead to resistance in humans (Bungau et al., 2021). Due to the widespread occurrence of antibiotic resistance in the animals, and environment, the risk of transmission of antibiotic resistance to humans is increasing. There is an urgent need to take action to reduce the use of antibiotics to limit the emergence and spread of drug-resistant bacteria in the environment, in animals and the food chain, thereby minimizing the associated threat to public health (Hu and Cheng, 2016; Hu et al., 2017).

*Aeromonas hydrophila* is a parthenogenetic anaerobic oxidative organic heterotrophic bacterium that causes gastroenteritis and

* Corresponding author at: State Key Laboratory of Marine Environmental Science, College of Ocean & Earth Sciences, Xiamen University, Xiamen, Fujian 361102, China.
*E-mail addresses:* chenfangyi@xmu.edu.cn (F. Chen), wkjian@xmu.edu.cn (K.-J. Wang).

https://doi.org/10.1016/j.aquaculture.2024.741137
Received 6 February 2024; Received in revised form 20 May 2024; Accepted 22 May 2024
Available online 24 May 2024

septicemia in fish and a disease named motile Aeromonas septicemia (MAS) (Semwal et al., 2023; Stratev and Odeyemi, 2016). *A. hydrophila* infection leads to a systemic inflammatory response (SIRS) (Claudiano et al., 2019), and the consequences of this uncontrolled inflammatory response are multi-organ pathology and high mortality rates (Liu et al., 2020). *A. hydrophila* is capable of causing pathogenicity in a wide range of mariculture and freshwater aquaculture species, including mandarin fish (*Siniperca chuatsi*) (Gao et al., 2024; Liu et al., 2020), Nile tilapia (*Oreochromis niloticus*) (Tartor et al., 2021), Crucian carp (*Carassius auratus*) (Xiong et al., 2022), *etc.* In the case of tilapia, for example, the mortality rate of infected fish is 35–50% (Tartor et al., 2021). With the expansion of aquaculture, high-density farming has led to the occurrence of many bacterial diseases and increased use of antimicrobial drugs. Misuse of antibiotics to avoid and treat fish diseases will lead to accelerated emergence of antibiotic-resistant strains (Rhodes et al., 2000) and unacceptable levels of drug residues in aquaculture products (Rahman et al., 2010). Among these diseases, septicemia caused by *A. hydrophila* is a serious disease that requires treatment with a wide range of antibiotics such as ampicillin, amoxicillin, gentamicin, streptomycin, trimethoprim, sulfamethoxazole, chloramphenicol, colistin, and erythromycin (Daood, 2012; Tartor et al., 2021). Multi-resistant *A. hydrophila* isolated from around the world have been accounted for to be impervious to penicillin and ampicillin (Igbinosa et al., 2012). To promote and accelerate the development of aquaculture, it is necessary to foster new antimicrobial agents that are safe, and free of harmful residues.

It is well known that AMPs are expected to replace antibiotics as effective therapeutic agents against pathogens. AMP as an important component of the innate immune system is considered the first line of defense against pathogenic microbial infections that can alter the cellular function of microorganisms by binding to membrane and/or cytoplasmic components, leading to cell death or metabolic exhaustion (Corrêa et al., 2019; Nordstrom et al., 2018). The characteristics of AMPs, including their amino acid composition, amphiphilicity, charge, *etc.*, contribute to their ability to insert into lipid bilayers and subsequently form pores and cellular extravasation (Ciumac et al., 2019). In addition, AMPs may inhibit the synthesis of various cellular components as well as enzymatic functions of the target cell (Malekkhaiat Häffner and Malmsten, 2018; Zhou et al., 2019). AMPs are ideal alternatives to antibiotics. As a bio-endogenous active molecule, AMPs are chemically degradable by proteases in the digestive system without harmful residues (Ji et al., 2024). In addition, AMPs are also more readily degraded in the environment than traditional antibiotics, which have low degradability, and do not cause secondary problems such as contamination, bacterial resistance or ecosystem damage (Correia et al., 2017). AMPs act on the conserved components of the cell membrane structure, and their rapid and efficient membrane-disrupting mechanism make it necessary for the bacteria to undergo a long period of mutagenesis to fully restore the cell membrane structure, thus greatly reducing the probability of bacteria developing resistance (Greber et al., 2020).

Intriguingly, almost all organisms possess AMPs as part of the evolutionarily conservation of innate immunity (De Santis et al., 2017). Marine invertebrates, with their enormous genetic diversity and biodiversity, have proven to be a rich source for the discovery of novel and potent AMPs (Sperstad et al., 2011). Mud crab (*Scylla paramamosain*) is an economically important aquaculture species worldwide, mainly distributed in the Indo-West Pacific region. In China, mud crab aquaculture has been developing rapidly, and mud crabs have become a major mariculture species (Chen and Wang, 2019). In 2022, mud crab aquaculture production in China is 154,661 t and 69,025 t from fishing (Wang et al., 2023). Mud crabs belong to invertebrates and thus can only rely on the innate immune system to protect against exogenous microbial infections, of which AMPs are key components and play an important role in immune defense. Mud crabs undergo multiple molts (>20) throughout their lifetime, when they usually stop feeding, and are susceptible to microbial infections at such a vulnerable developmental stage. These unique characteristics of mud crabs imply that it is possible to identify a variety of novel AMPs from these marine crabs living in such a complex environment.Our laboratory has identified a variety of AMPs with potent antimicrobial activity, some of which have good *in vitro* activity against *A. hydrophila*, such as Scyreptin$_{1–30}$ (Zhang et al., 2023) and Sparanegtin (Zhu et al., 2021). However, the *in vivo* antimicrobial activity of the above AMPs against *A. hydrophila* has not been revealed. In recent years, there has been increasing interest in developing new AMPs as antibiotic alternatives against pathogenic infections, but studies on AMPs against *A. hydrophila* diseases is still scarce (Gao et al., 2024).

In this study, we identified a new functional gene, named Spasin, based on the analysis of the constructed transcriptome database of *S. paramamosain* after bacterial challenge. The full-length cDNA of Spasin was obtained by RACE PCR and its expression profiles were analyzed in various tissues of adult crabs and at different developmental stages of crabs. In addition, by analyzing the physicochemical properties of AMP and the predictions of the AMP database, we obtained the truncated peptide Spasin$_{141–165}$ derived from Spasin and determined the antimicrobial activity of its chemically synthesized peptide. The *in vitro* antimicrobial mechanism of Spasin$_{141–165}$ was further investigated, and its *in vivo* effect against *A. hydrophila* was revealed using a zebrafish bacterial infection model. The qPCR method used in this study was to detect the transcriptional expression level of Spasin in tissues by absolute quantitative PCR and to detect the expression level of inflammatory cytokines in zebrafish spleen tissues by relative quantitative. This study aimed to characterize the physicochemical properties and antimicrobial activity of the novel AMP Spasin$_{141–165}$, to elucidate its antimicrobial effect against *A. hydrophila* infection and its intrinsic mechanism, and thus to develop a potentially effective antimicrobial agent which could be used as an alternative to antibiotics for future applications in aquaculture.

## 2. Materials and methods

### 2.1. Animals, cell lines, and microorganisms

Mud crabs (*S. paramamosain*) (approx. 300 g ± 10 g) were purchased from a crab farm in Zhangpu (Zhangzhou, China), and acclimatized for at least three days prior to the experiments. Healthy adult male and female mud crabs were dissected and tissues from hemocytes, muscle, gills, subcuticular epidermis, anterior vas deferens, eye stalk, seminal vesicle, heart, ejaculatory duct, stomach, thoracic ganglion mass, testis, posterior vas deferens, posterior ejaculatory duct (including androgenic gland), midgut, hepatopancreas, ovary, reproductive tract, spermathecae, and brain were collected. The different developmental stages of crabs, including embryos I-V, zoea I-V, megalopa, and juvenile crab, were sampled.

Wild-type zebrafish (*Danio rerio*) AB strain (approx. 0.5 g) was purchased from the China Zebrafish Resource Center (Wuhan, China). Throughout the experiment, all fish were kept in a recirculating freshwater aquarium at 26 °C–28 °C and fed twice daily with brine shrimp. Fish were anesthetized with 0.4% ethyl 3-aminobenzoate methanesulfonate (MS222, Sigma-Aldrich, USA) before injection, followed by tissue sampling. Approved by the Experimental Animal Ethics Committee of Xiamen University (No. XMULAC20240082), all experimental designs and manipulations were guided by local guidelines for the use of research animals.

The HEK293T cell line was purchased from the National Collection of Authenticated Cell Cultures (Shanghai, China) and cultured in DMEM (Gibco, USA) medium supplemented with 10% fetal bovine serum (Gibco, USA) at 37 °C under 5% $CO_2$. The zebrafish embryonic fibroblast cell line (ZF4) was bought from the China Zebrafish Resource Center (Wuhan, China) and cultured in DMEM-F12 (1:1) (Gibco, USA) medium supplemented with 10% fetal bovine serum (Gibco, USA) at 28 °C under 5% $CO_2$. We purchased strains from the China General Microbiological

Culture Collection Center (CGMCC), including *Micrococcus luteus* (CGMCC No. 1.2299), *Micrococcus lysodeikticus* (CGMCC No. 1.634), *Enterococcus faecium* (CGMCC No. 1.131), *Bacillus subtilis* (CGMCC No. 1.3358), *Corynebacterium glutamicum* (CGMCC No. 1.1886), *Staphylococcus aureus* (CGMCC No. 1.2465 and CGMCC No. 11.879), *Pseudomonas stutzeri* (CGMCC No. 1.1803), *Acinetobacter baumannii* (CGMCC No. 1.6769), *Pseudomonas fluorescens* (CGMCC No. 1.3202), *Shigella flexneri* (CGMCC No. 1.1868), *Escherichia coli* (CGMCC No. 1.2389), *A. hydrophila* (CGMCC No. 1.2017), *Fusarium solani* (CGMCC No. 3.584), *Fusarium oxysporum* (CGMCC No. 3.6785), *Fusarium graminearum* (CGMCC No. 3.4521), and *Aspergillus niger* (CGMCC No. 3.316).

### 2.2. Gene cloning, sequence analysis and qPCR

Using our laboratory's previously established database of mud crab transcriptomes following *Vibrio alginolyticus* challenge, we succeeded in identifying a significantly upregulated uncharacterized gene. Based on the predicted sequences, we designed specific primers to amplify the full length cDNA sequence of the gene. The primers were listed in Supplementary Table 1. A mixture of cDNAs generated from different tissues was used as a template. We predicted the physicochemical properties of amino acid sequences through the ExPASy website (https://www.expasy.org/). Similarity analysis of amino acid and nucleotide sequences was calculated using the DNAMAN software (Version 6.0). Genomic data from the NCBI database (https://www.ncbi.nlm.nih.gov/) was downloaded for gene homology analysis.

Total RNA from tissue samples was extracted using TRIzol reagent (Thermo Fisher, USA). 1 mL of tissue lysate was added to 200 μL of chloroform and vortexed for 30 s. The upper phase was carefully transferred to a new 1.5 mL tube and an equal volume of isopropanol was added. The tube was then inverted several times to mix the solutions, allowed to stand at room temperature for 15 min, and centrifuged at 13,000 rpm for 15 min at 4 °C. The supernatant was discarded and the RNA was washed twice with 1 mL of 75% ethanol. The RNA was dried briefly at room temperature and dissolved in RNase-free water. RNA concentration was quantified using a NanoDrop 2000 spectrophotometer (Thermo Fisher, USA). Total RNA from each sample was extracted and cDNA was synthesized, followed by verification of primer specificity. Primers used for qPCR analysis is shown in Supplementary Table 1. Spasin expression levels were detected using FastStart DNA Master SYBR Green I (Roche, Germany) in a real-time thermocycler (ABI 7500, Waltham, USA) with cDNA as a template. The expression profiles of the Spasin gene were determined by absolute quantitative real-time PCR (qPCR) at different developmental stages and in different tissues of adult crabs. The absolute mRNA expression copies $mL^{-1}$ was calculated as follows: Spasin fragments (the product of qPCR) were inserted into the pMD 18-T plasmid, the recombinant plasmid was purified and its concentration was determined, and the copy number of the recombinant plasmid was calculated according to the following formula (Whelan et al., 2003).

$$\text{Weight in daltons}\left(\text{g mol}^{-1}\right) = (\text{bp size of ds product})\left(330\,\text{Da} \times 2\,\text{nt bp}^{-1}\right)$$

$$\text{Hence}: \left(\text{g mol}^{-1}\right)/\text{A vogadro}^{'}\text{s number} = \text{g molecule}^{-1} = \text{copy number}$$

$$(\text{where}: \text{bp} = \text{base pair}, \text{ds} = \text{double stranded}, \text{nt} = \text{nucleotide}).$$

Gradient dilution of the recombinant plasmid was performed, and the CT value of each sample was tested separately, and a standard curve was plotted according to the correspondence between CT values (y) and the logarithm of the copy number (x):

$$y = -3.149 \times +31.65$$

$$R^2 = 0.9949$$

Finally, the copy number for each sample was calculated according to the standard curve. Divide the calculated copy number by the volume of the sample solution to obtain the copies $mL^{-1}$.

### 2.3. Peptide design and synthesis

The amino acid sequence of Spasin was analyzed using the Collection of Anti-Microbial Peptides ($CAMP_{R3}$) (http://www.camp.bicnirrh.res.in/) to predict fragments with possible antimicrobial activity. $Spasin_{141–165}$ (KKLGKIPEKKHKVKSKVVASCSGLP) derived from Spasin was chemically synthesized by Genscript (Nanjing, China) with >95% purity. Briefly, solid-phase-peptide synthesis uses a solid support material such as polystyrene resin to bind and immobilize the synthesized peptide. During the synthesis process, the N-terminus or side chain of the peptide is chemically modified with a protecting group. Further modifications include coupling reagents and linkers, which facilitate the sequential addition of amino acids. The C-terminus of the first AA is covalently attached to the solid-phase resin so that the peptide can be synthesized in the C—N direction (Deo et al., 2022).

### 2.4. Antimicrobial assay

The antimicrobial activity of $Spasin_{141–165}$ was determined using a slightly modified broth microdilution assay (Shan et al., 2016). Briefly, bacteria in logarithmic growth phase were diluted to approximately $10^6$ colony forming units (CFU) per milliliter with Muller-Hinton broth (HKM, China), were incubated in 96-well flat-bottomed plates (NEST, China), mixed with different concentrations of peptides (1.5 to 96 μM) at 37 °C for 24 h. Meanwhile, LL-37 (Jill Biochemistry, China) and Milli-Q water were set up as controls, respectively. The lowest concentration at which there was no visible bacterial growth was recorded as the minimum inhibitory concentration (MIC); the lowest peptide concentration that killed ≥99.9% of bacteria was recorded as the minimum bactericidal concentration (MBC). This assay was carried out in triplicate at least three times.

### 2.5. Time-killing kinetic assay

*S. aureus* and *A. baumannii* were selected for the time-killing kinetic assay with the methodology referring to what has been reported (Shan et al., 2016). Briefly, bacteria in logarithmic growth phase were diluted to ~$10^6$ CFU $mL^{-1}$ with MH medium and then mixed in equal volume with $Spasin_{141–165}$ (1 × MIC) and incubated at 37 °C. Samples were taken at 0, 5, 10, 15, 20, 25, 30, 45, 60, 90, 120 and 150 min at intervals, and were spread evenly on NB agar plates and incubated at 37 °C for 24 h.The number of survivors was then quantified, while the peptide-free medium was used as a control. This assay was carried out in triplicate at least three times.

### 2.6. Scanning electron microscope (SEM) observation

The effect of $Spasin_{141–165}$ on *S. aureus* and *A. baumannii* was observed using SEM according to a previous method (Wang et al., 2022). Resuspend the logarithmic growth phase of *S. aureus* and *A. baumannii* to approximately 1 × $10^8$ CFU $mL^{-1}$ with 10 mM NaPB and then incubated with $Spasin_{141–165}$ (1 × MIC) for 30 min at room temperature. Afterward, the samples were then fixed overnight with 2.5% (*v*/v) glutaraldehyde; the samples were then washed and resuspended in NaPB and deposited on glass slides at 4 °C. Next, cells were dehydrated with ethanol and then dried in a critical point dryer (EM CPD300, Leica, Germany). Finally, the samples were examined using a scanning electron microscope (Zeiss SUPRA 55, Germany) after coating with gold.

### 2.7. Transmission electron microscope observation

TEM analyses were performed according to the reported

experimental methods (Zhu et al., 2021). Briefly, *S. aureus* and *A. baumannii* were incubated with $Spasin_{141–165}$ for 30 min, respectively. The cells were rinsed with NaPB and added to the agar model. The samples were then fixed with 2.5% glutaraldehyde overnight. After that, they were rinsed with NaPB for 15 min and repeated three times, then post-fixed with 1% osmium tetroxide, dehydrated and rinsed, embedded in epoxy resin, and observed under a transmission electron microscope (HT7800, Hitachi, Japan).

### 2.8. Thermal stability and cation tolerance assay

*S. aureus* and *A. baumannii* were selected to evaluate the thermoactivity of $Spasin_{141–165}$, and the methodology was referenced from a previous report (Jiang et al., 2022). Briefly, *S. aureus* and *A. baumannii* in logarithmic growth phase were diluted to approximately $1 \times 10^7$ CFU $mL^{-1}$. $Spasin_{141–165}$ was treated at 100 °C for 30, 60, 90, and 120 min, or at different temperatures (4, 16, 28, 37, 50, 80, 100, and 121 °C) for 60 min, respectively, and then returned to room temperature. The different groups of $Spasin_{141–165}$ were incubated with bacteria in microtiter plates at 37 °C overnight.

Similarly, in cation tolerance experiments, prepared bacteria were mixed with $Spasin_{141–165}$ spiked with different concentrations of cationic salt solutions ($Na^+$ 50 to 500 mM, $K^+$ 2 to 10 mM), added to the wells and incubated at 37 °C overnight. The above experiment was performed using a microplate reader (Tecan, Switzerland) to measure absorbance at 600 nm. This assay was carried out in triplicate at least three times.

### 2.9. Cytotoxicity and hemolysis assay

The cytotoxicity of $Spasin_{141–165}$ on cell lines including HEK-293 T, RAW 264.7, and ZF4 was assessed by MTS assay as previously described (Yang et al., 2020). In brief, the density of the human embryonic kidney cells (HEK-293 T), mouse macrophages (RAW 264.7), and zebrafish embryonic fibroblasts (ZF4) were adjusted to approximately $1 \times 10^5$ cells $mL^{-1}$ and cultured in a 5% $CO_2$ atmosphere incubator overnight at 37 °C and 28 °C, respectively. The medium was then removed and supplemented with various concentrations of peptides (0, 6, 12, 24, and 48 μM) in fresh medium and incubated for 24 h. Similarly, the hemolytic activity of $Spasin_{141–165}$ was determined using mouse erythrocytes. Finally, cell viability was determined using the CellTiter 96® AQueous kit (Promega, USA). This assay was carried out in triplicate at least three times.

### 2.10. Lipoteichoic acid and lipopolysaccharides inhibition assays

25 μL of lipoteichoic acid (LTA) (8 to 64 mg $mL^{-1}$) from *S. aureus* (Sigma, USA) or 25 μL of lipopolysaccharides (LPS) (8 to 64 mg $mL^{-1}$) from *E. coli* (Sigma, USA) were added to a 96-well flat-bottomed plate containing 25 μL of $Spasin_{141–165}$ (1 × MIC), and allowed to stand for 30 min at room temperature. Subsequently, 50 μL of *S. aureus* ($1 \times 10^6$ CFU $mL^{-1}$) or 50 μL of *A. baumannii* ($1 \times 10^6$ CFU $mL^{-1}$) cells were added to the wells and incubated with $Spasin_{141–165}$-LTA mixture or $Spasin_{141–165}$-LPS, respectively, incubated at 37 °C for 24 h and using a microplate reader (Tecan, Switzerland) to measure the absorbance at 595 nm. This assay was carried out in triplicate at least three times.

### 2.11. ROS measurement

*S. aureus* and *A. baumannii* were incubated in NB medium at 37 °C overnight. The bacteria were then washed with NaPB and the suspension was diluted to a concentration of approximately $1 \times 10^7$ CFU $mL^{-1}$ before adding a final concentration of 10 mM of the fluorescent probe 2′,7′-dichlorofluorescein diacetate (DCFH-DA) (R&D, USA). The mixture was then mixed with 50 μL of $Spasin_{141–165}$ (1 × MIC) or polymyxin B (20 μg $mL^{-1}$) in equal volumes, added to a 96-well flat-bottomed plate, and incubated at 37 °C for 30 min protected from light. Immediately after incubation, relative levels of ROS were measured continuously at 510 nm absorbance using a microplate reader (Tecan, Switzerland). This assay was carried out in triplicate at least three times.

### 2.12. ATP release

*S. aureus* and *A. baumannii* cells were washed with NaPB and resuspended to approximately $10^7$ CFU $mL^{-1}$. Subsequently, an equal volume of $Spasin_{141–165}$ was added and incubated for 30 min at 37 °C. Subsequently, luciferin-luciferase was added to the mixture according to the instructions of the ATP Assay Kit (Invitrogen, USA) and fluorescence was detected using a Glo-Max™ 20/20 Fluorometer (Promega, USA). A standard curve was plotted to calculate the extracellular ATP concentration. This assay was carried out in triplicate at least three times.

### 2.13. Outer membrane permeability assay

Evaluation of bacterial outer membrane permeability by uptake assay with *N*-phenyl-1-naphthylamine (NPN) (Sigma-Aldrich, USA). Logarithmic-growth phase cultured *S. aureus* and *A. baumannii* cells were washed with NaPB. Cells were resuspended in 5 mM HEPES buffer (pH 7.4, containing 5 mM glucose) to approximately $10^8$ CFU $mL^{-1}$. A final concentration of 10 μM NPN was added to the bacterial suspension, and the mixture was placed into a 96-well, black, flat-bottomed microtiter plate and incubated for 5 min at room temperature, protected from light. The mixture was then incubated with different concentrations of $Spasin_{141–165}$ (24 μM and 48 μM). As positive controls, LL-37 (24 μM, Jill Biochem, China) and polymyxin B (PMB, 20 μg $mL^{-1}$, Solarbio, China) were used. Fluorescence intensity (excitation 350 nm, emission 420 nm) was recorded every 2 min using a microplate reader (Tecan, Switzerland).This assay was carried out in triplicate at least three times.

### 2.14. Membrane permeability assay

The effect of $Spasin_{141–165}$ on membrane permeability was tested by reference to the method of the LIVE/DEAD BacLight™ Bacterial Viability Kit (Thermo Fisher, USA). *S. aureus* and *A. baumannii* cells were conditioned to approximately $10^7$ CFU $mL^{-1}$ with sterile NaPB and then mixed with different concentrations of $Spasin_{141–165}$ (12 μM and 24 μM), respectively. As positive controls, LL-37 (24 μM, Jill Biochem, China) and polymyxin B (PMB, 20 μg $mL^{-1}$, Solarbio, China) were used. After incubation, the cells were washed twice with PBS and then stained with SYTO 9 and PI for 15 min under light-free conditions. Finally, fluorescence images were acquired using a confocal laser scanning microscope (Zeiss, Germany).

### 2.15. Evaluation of the in vivo protective effect of $Spasin_{141–165}$ on *A. hydrophila* infected zebrafish

In this study, we investigated the *in vivo* anti-infective effect of $Spasin_{141–165}$ by constructing a model of adult zebrafish infected with *A. hydrophila*. Briefly, zebrafish were randomized divided into four groups ($n$ = 40, female:male = 1:1). Logarithmic growth phase of *A. hydrophila* were washed three times with fish saline, and the final concentration was adjusted to $2.3 \times 10^8$ CFU $mL^{-1}$. Zebrafish were given an intraperitoneal injection of bacterial suspension, 8.8 μL per fish, followed 1 h later by an injection of $Spasin_{141–165}$ (1 mg $mL^{-1}$), 8.8 μL per fish. In addition, fish saline was injected 1 h after an injection of *A. hydrophila* ($10^6$ CFU/fish) as a control group. Mortality of each group of fish was monitored and recorded at 2-h intervals and the survival curve was drawn with GraphPad Prism 9.0.0 version (San Diego, CA, USA).

Zebrafish spleens collected at the last time point were weighed and homogenized in sterile PBS. Tissue homogenates were spread evenly on nutrient agar plates after gradient dilution and incubated at 37 °C for 24

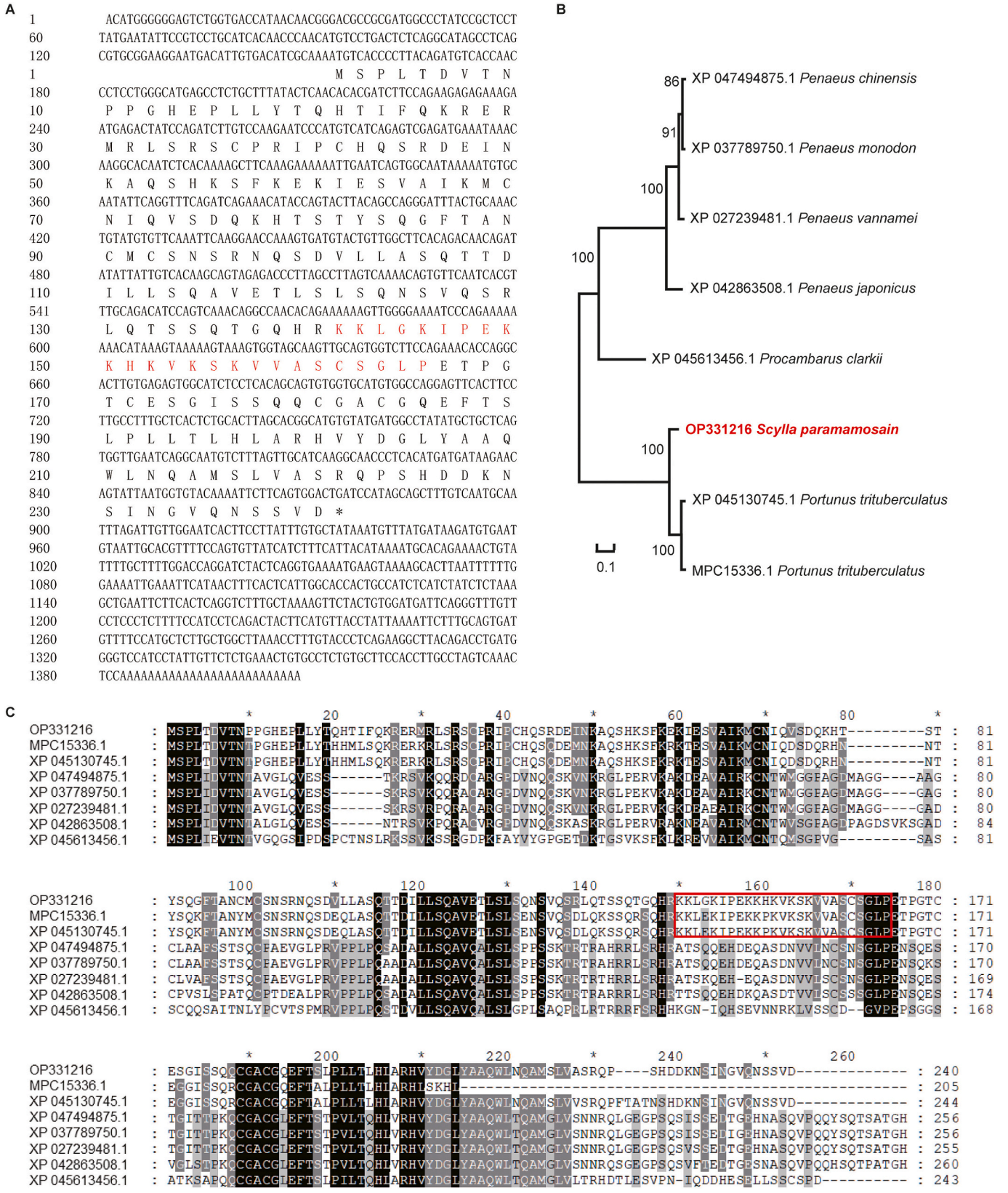


**Fig. 1.** Full-length cDNA and amino acid sequence of Spasin, phylogenetic tree analysis, and multiple alignment of homologous genes with other species. (A) The full-length cDNA sequences of Spasin and its predicted amino acid sequences. (B) Phylogenetic tree analysis of Spasin. A neighbor-joining phylogenetic tree was constructed using MEGA ver.5.0 software with 3000 bootstrap replications. (C) Multiple alignment of Spasin amino acid sequences with homologous genes from other species. The boxed region represents the amino acid sequence of Spasin$_{141–165}$ (red). (For interpretation of the references to colour in this figure legend, the reader is referred to the web version of this article.)

**Table 1**
Sequence information and physicochemical properties of Spasin.

| Physicochemical parameters | Spasin |
|---|---|
| Number of amino acids | 240 |
| Molecular MW (Da) | 26,494.89 |
| Theoretical PI | 9.07 |
| Formula | $C_{1127}H_{1835}N_{343}O_{366}S_{14}$ |
| Total number of atoms | 3685 |
| Grand average of hydropathicity | −0.617 |

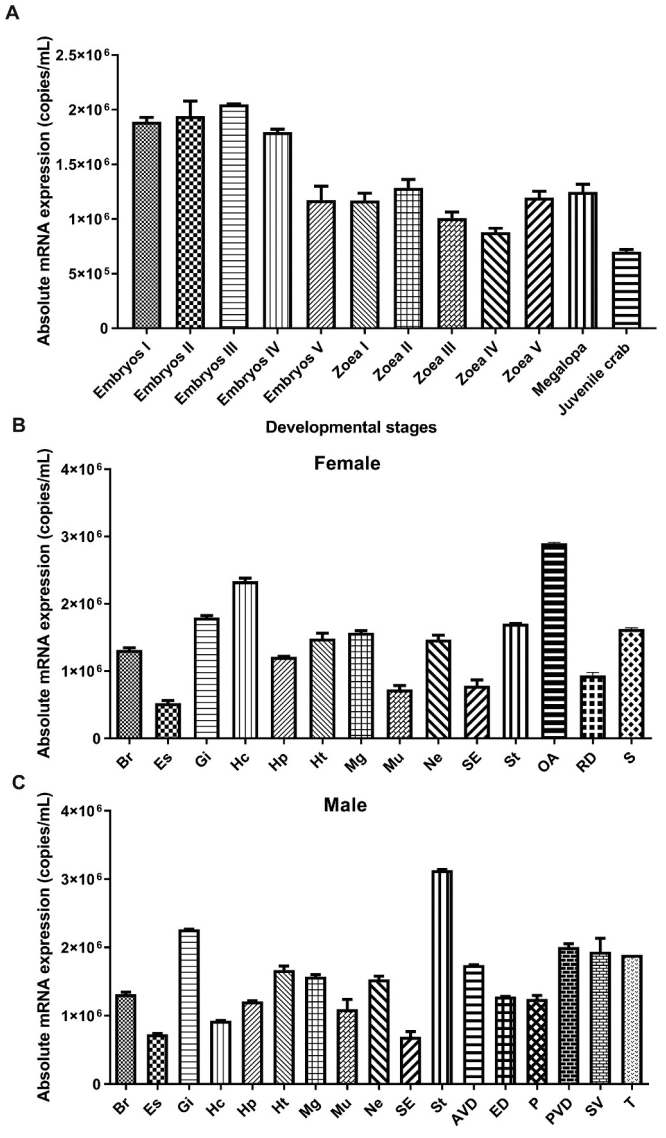


**Fig. 2.** Expression profiles of Spasin in *S. paramamosain*. Tissue distribution of Spasin was detected in different developmental stages of crabs (A), adult female (B), and male (C) crabs ($n = 3$). Hc, hemocytes; Mu, muscle; Gi, gill; Se, subcuticular epidermis; Es, eye stalk; Ht, heart; St, stomach; Ne, thoracic ganglion mass; T, testis; AVD, anterior vas deferens; SV, seminal vesicle; PVD, posterior vas deferens; ED, ejaculatory duct; P, posterior ejaculatory duct (including androgenic gland); Mg, midgut; Hp, hepatopancreas; OA, ovary; RD, reproductive tract; S, spermathecae; and Br, brain.

h. CFUs were subsequently counted. Changes in the expression of inflammation-associated factors following Spasin treatment of *A. hydrophila*-challenged zebrafish were analyzed by relative qPCR with EF1α as an internal reference gene, and the expression profile analysis was carried out using $2^{-\Delta\Delta Ct}$ algorithm (Livak and Schmittgen, 2001). The experiments were performed twice independently.

### 2.16. Statistical analysis

Statistical analyses were performed using GraphPad PRISM ver. 5.0 (GraphPad Software, Inc.) and the SPSS 18.0 software package (SPSS Inc.). One-way ANOVA analysis was used to compare the data of each group. $p$-value $<0.05$ was considered statistically significant.

## 3. Results

### 3.1. Sequence analysis of Spasin gene

We obtained the full-length cDNA of a new functional gene, named Spasin (Genbank accession number OP331216), by RACE PCR based on the mud crab (*S. paramamosain*) transcriptomic database constructed in our laboratory. This gene consists of a 152 bp 5′ UTR, a 533 bp 3′ UTR, and a 723 bp ORF (Fig. 1A). The Spasin ORF encodes a 240-amino acid protein with sequence similarity and high homology to two uncharacterized functional genes of *Portunus trituberculatus* (Genbank accession number: XP 045130745.1 and MPC15336.1), and their amino acid identity were 86.7% and 84.4% (Supplementary Table 2), respectively. Phylogenetic analysis showed that these genes were clustered into the same branch (Fig. 1B & 1C). Spasin is a cationic protein with a calculated molecular weight of 26.50 kDa and an estimated isoelectric point (pI) of 9.07 (Table 1).

### 3.2. Tissue distribution and expression profiles of Spasin

The expression profiles of Spasin in mud crabs at different developmental stages were examined (Fig. 2A). The qPCR results showed that Spasin was distributed in different developmental stages of mud crabs, among which the expression of Spasin was relatively high in embryonic stages I-IV, about $1.8 \times 10^6$ copies $mL^{-1}$. In addition, Spasin gene was distributed in different tissues of adult crabs, among which the highest expression of Spasin was found in the ovaries of female adult crabs (about $3 \times 10^6$ copies $mL^{-1}$) (Fig. 2B), while in male adult crabs, Spasin was mainly expressed in the stomach (about $3.2 \times 10^6$ copies $mL^{-1}$) (Fig. 2C).

### 3.3. Truncated peptide design and antimicrobial activity analysis

The truncated peptide $Spasin_{141–165}$ (located at amino acids 141–165 of the mature peptide of Spasin) was designed and predicted according to the AMP database CAMPR3, and its sequence and main physicochemical parameters are shown in Table 2. $Spasin_{141–165}$ consists of 25 amino acid residues, has a calculated mass of 2690.33 Da, a hydrophobicity ratio of 14.4% and an estimated pI of 10.24. The total net charge is +7. Information about the other two AMPs LL-37 an HBD-2 is listed in Table 2. All three peptides have an amino acid length of <50 residues, a hydrophobicity between 14% and 49%, a net charge between +6 and + 7, and similar theoretical pI.

The results showed that $Spasin_{141–165}$ exhibited a broad spectrum of antimicrobial activity. The measured MIC and MBC values are summarized in Table 3. $Spasin_{141–165}$ significantly inhibited several Gram-positive bacteria, such as *Micrococcus luteus*, *Micrococcus lysodeikticus*, *Enterococcus faecium*, *Bacillus subtilis*, *Corynebacterium glutamicum*, and *Staphylococcus aureus*, as well as Gram-negative bacteria, such as *Pseudomonas stutzeri*, *Acinetobacter baumannii*, *Pseudomonas fluorescens*, *Shigella flexneri*, and *Escherichia coli*, with the MIC values in the range of 0.75–48 μM, and the MBC values lower than 48 μM. In addition, $Spasin_{141–165}$ exhibited antifungal conidial germination activity against several filamentous fungi, including *Fusarium solani*, *Fusarium oxysporum*, *Fusarium graminearum*, and *Aspergillus niger*, with MIC values ranging from 0.75 to 48 μM.

**Table 2**
The key physicochemical parameters of Spasin$_{141–165}$, LL-37, and HBD-2.

| Physicochemical parameters | Spasin$_{141–165}$ | LL-37 | HBD-2 |
|---|---|---|---|
| Sequence | KKLGKIPEKKHKVKSKVVASCSGLP | LLGDFFRKSKEKIGKEFKRIVQRIKDFLRNLVPRTES | GIGDPVTCLKSGAICHPVFCPRRYKQIGTCGLPGTKCCKKP |
| Number of amino acids | 25 | 37 | 41 |
| Molecular MW (Da) | 2690.33 | 4493.22 | 4334.24 |
| Theoretical PI | 10.24 | 10.61 | 9.30 |
| Formula | $C_{121}H_{217}N_{35}O_{31}S_1$ | $C_{205}H_{340}N_{60}O_{53}$ | $C_{188}H_{311}N_{55}O_{50}S_6$ |
| Hydrophobic residue% | 14.4% | 20.1% | 48.9% |
| Hydrophobic moment | 0.422 | 0.521 | 0.246 |
| Grand average of hydropathicity | −0.612 | −0.724 | −0.102 |
| Total net charge | +7 | +6 | +6 |

**Table 3**
Antimicrobial activity of Spasin$_{141–165}$.

| Microorganisms | CGMCC No.[a] | MIC[b] (μM) | MBC[c]/MFC[d] (μM) |
|---|---|---|---|
| Gram-positive bacteria | | | |
| *Micrococcus luteus* | 1.2299 | 0.75–1.5 | 0.75–1.5 |
| *Micrococcus lysodeikticus* | 1.634 | 0.75–1.5 | 0.75–1.5 |
| *Enterococcus faecium* | 1.131 | 0.75–1.5 | 0.75–1.5 |
| *Bacillus subtilis* | 1.3358 | 0.75–1.5 | 0.75–1.5 |
| *Corynebacterium glutamicum* | 1.1886 | 1.5–3 | 3–6 |
| *Staphylococcus aureus* | 1.2465 | 24–48 | 24–48 |
| *Staphylococcus aureus* | 1.879 | 24–48 | 24–48 |
| Gram-negative bacteria | | | |
| *Pseudomonas stutzeri* | 1.1803 | 6–12 | 12–24 |
| *Acinetobacter baumannii* | 1.6769 | 12–24 | 24–48 |
| *Pseudomonas fluorescens* | 1.3202 | 12–24 | 24–48 |
| *Shigella flexneri* | 1.1868 | 24–48 | 24–48 |
| *Escherichia coli* | 1.2389 | 24–48 | 24–48 |
| *Aeromonas hydrophila* | 1.2017 | >48 | >48 |
| *Edwardsiella tarda* | | >48 | >48 |
| Fungi | | | |
| *Fusarium solani* | 3.584 | 0.75–1.5 | 3–6 |
| *Fusarium oxysporum* | 3.6785 | 1.5–3 | 1.5–3 |
| *Fusarium graminearum* | 3.4521 | 3–6 | 3–6 |
| *Aspergillus niger* | 3.316 | 24–48 | >48 |

[a] China General Microbiological Culture Collection Center.
[b] The values of MIC were expressed as the interval [a]-[b]. [a] was the highest concentration tested with visible microbial growth, whereas [b] was determined as the lowest concentration without visible microbial growth.
[c] The values of MBC presented are those wherein the peptide concentration killed 99.99% of the bacteria.
[d] The values of MFC presented are those wherein the peptide concentration killed 99.99% of the fungi.

### 3.4. Bactericidal kinetics of Spasin$_{141–165}$

*S. aureus* and *A. baumannii* were selected for bactericidal kinetic assay to evaluate the bactericidal efficacy of Spasin$_{141–165}$. When incubated with *S. aureus* or *A. baumannii*, Spasin$_{141–165}$ at 1 × MBC killed 99.9% bacteria within 2 h or 90 min, respectively (Fig. 3A&3B).

### 3.5. Morphological changes in Spasin$_{141–165}$ treated bacteria

SEM and TEM were carried out to observe the morphological changes of the bacteria *S. aureus* and *A. baumannii* after Spasin$_{141–165}$ treatment. The results showed that after Spasin$_{141–165}$ treatment, the integrity of the cell membrane of the bacteria was disrupted and even leakage of cell contents (Fig. 3C&3D). In contrast, the surface of untreated cells was intact and smooth.

### 3.6. Effect of bacterial membrane components on the antibacterial activity of Spasin$_{141–165}$

Killing bacteria by binding to bacterial membrane surface components is a common antimicrobial mode of AMPs, where the major bacterial membrane components of Gram-positive and Gram-negative bacteria are LTA and LPS, respectively. In the study, the results showed that LTA and LPS inhibited the bactericidal effect of Spasin$_{141–165}$ against bacteria in a dose-dependent manner. As shown in Fig. 4A, the bactericidal effect of Spasin$_{141–165}$ was attenuated to varying degrees with exogenous addition of LTA (8, 16, 32, and 64 μg mL$^{-1}$). Similarly, addition of different concentrations of LPS (8, 16, 32, and 64 μg mL$^{-1}$) affected the bactericidal effect of Spasin$_{141–165}$ against *A. baumannii* (Fig. 4B). The results showed that the inhibitory activity of Spasin$_{141–165}$ against *S. aureus* or *A. baumannii* decreased with the increase of the concentration of LTA or LPS, suggesting that Spasin$_{141–165}$ might exert its inhibitory effect against Gram-positive or Gram-negative bacteria by binding to LTA or LPS.

### 3.7. Effect of Spasin$_{141–165}$ on bacterial membrane permeability

The increased fluorescence of the membrane non-permeable fluorescent dye NPN indicated that the bacterial outer membrane was damaged. As shown in Fig. 4C and D, the outer membrane of *S. aureus* or *A. baumannii* was disrupted and NPN was absorbed with a dose-dependent increase in fluorescence intensity after Spasin$_{141–165}$ treatment. On the other hand, the inner membrane permeability of *S. aureus* and *A. baumannii* after treatment with Spasin$_{141–165}$ was evaluated using SYTO 9 and propidium iodide (PI) staining. When bacteria were incubated with a mixture of SYTO 9 and PI, SYTO 9 labeled all bacteria, including both membrane-intact and membrane-damaged bacteria, whereas PI could only label membrane-damaged bacteria, resulting in a decrease in the fluorescence intensity of SYTO 9 staining. The results showed that, unlike the untreated group where almost all cells emitted green fluorescence, treatment of the bacteria with Spasin$_{141–165}$ resulted in a significant increase of red fluorescence (Fig. 5).

### 3.8. Spasin$_{141–165}$ induced intracellular ROS levels and ATP release

AMPs can exacerbate bacterial membrane damage by inducing ROS production (Oliveira et al., 2019). We examined ROS levels in *S. aureus* or *A. baumannii* cells after Spasin$_{141–165}$ treatment. As shown in Fig. 6A & 6B, Spasin$_{141–165}$ induced intracellular ROS production of both bacteria, and the accumulation increased with the concentration of treatment. In addition, we evaluated extracellular ATP levels after treatment of bacteria with different concentrations of Spasin$_{141–165}$. As shown in Fig. 6C & 6D, the Spasin$_{141–165}$-induced ATP release from *S. aureus* or *A. baumannii* cells after 30 min of incubation showed a concentration-dependent relationship with Spasin$_{141–165}$ concentration.

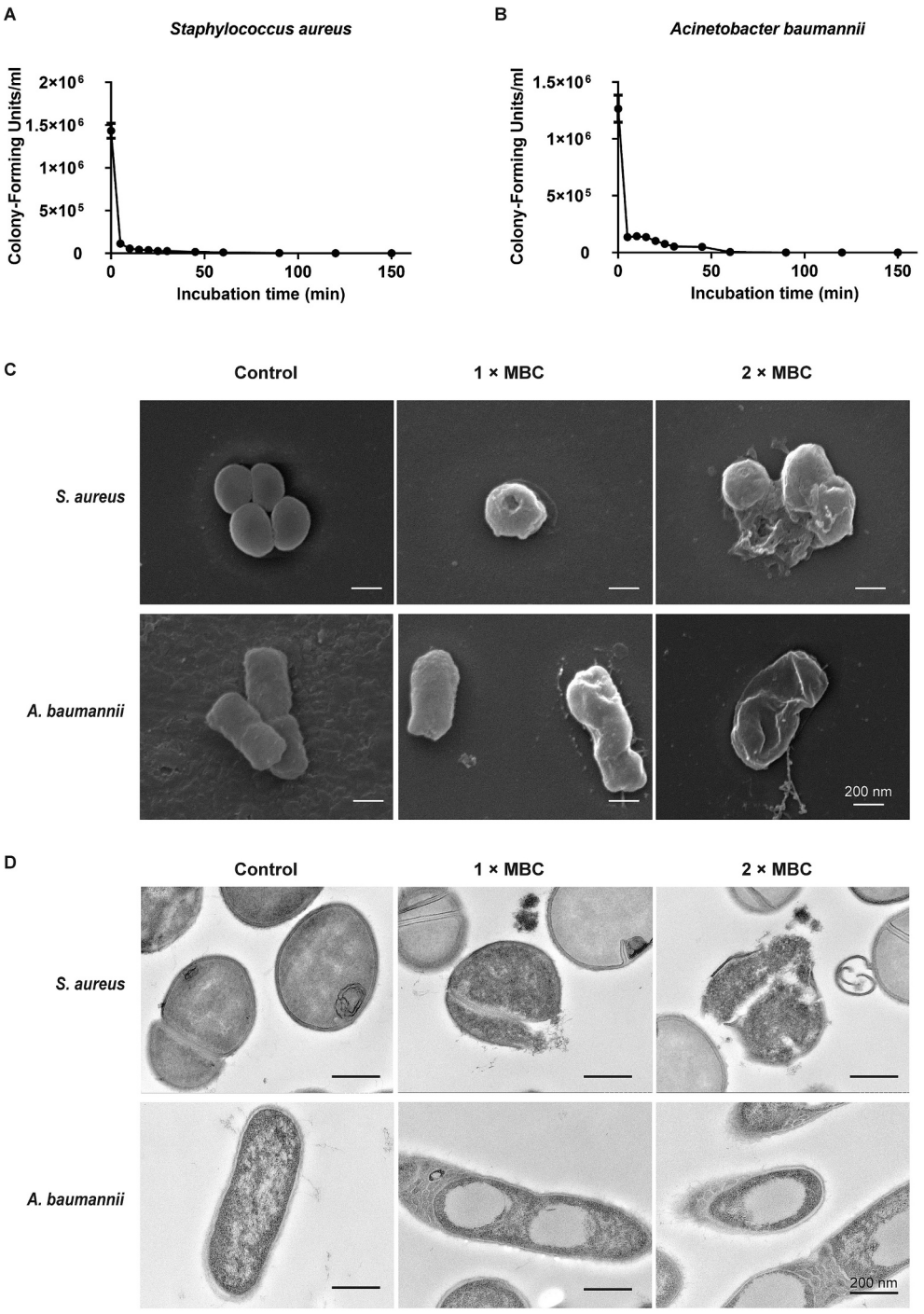


**Fig. 3.** Bactericidal kinetics of Spasin$_{141–165}$ against *S. aureus* (A)and *A. baumannii* (B) at 1× MBC. Data represent mean ± standard error of the mean from three independent biological replicates. Effect of Spasin$_{141–165}$ on morphological and structural changes of *S. aureus* and *A. baumannii* observed by SEM (C) and TEM (D).

### 3.9. The stability of Spasin$_{141–165}$

To evaluate the temperature tolerance of Spasin$_{141–165}$, we treated Spasin$_{141–165}$ at different temperatures for 30 min and then incubated with bacteria for 24 h. The results showed that the bactericidal activity of Spasin$_{141–165}$ against *S. aureus* and *A. baumannii* was retained (Fig. 7A & 7C). We further evaluated the effect of different treatment times at 100 °C on the bactericidal activity of Spasin$_{141–165}$ and the results showed that the bactericidal activity of Spasin$_{141–165}$ against *S. aureus* and *A. baumannii* was not affected after 2 h of continuous treatment (Fig. 7B & 7D). These results indicated that Spasin$_{141–165}$ had good thermal stability.

We also investigated the effect of different cation ($K^+$ and $Na^+$) concentration conditions on the sensitivity of bacteria to Spasin$_{141–165}$. We incubated Spasin$_{141–165}$ with bacteria at different concentrations of sodium, potassium, and magnesium ions for 24 h. The results showed that *S. aureus* and *A. baumannii* were still sensitive to Spasin$_{141–165}$ in 2 to 10 mM KCl solution (the $K^+$ concentration in natural seawater is approximately 10 mM) (Fig. 7E & 7F). *S. aureus* remained sensitive to Spasin$_{141–165}$ at 100 mM NaCl (Fig. 7G), while *A. baumannii* showed reduced susceptibility to Spasin$_{141–165}$ at 50 mM NaCl (Fig. 7H).

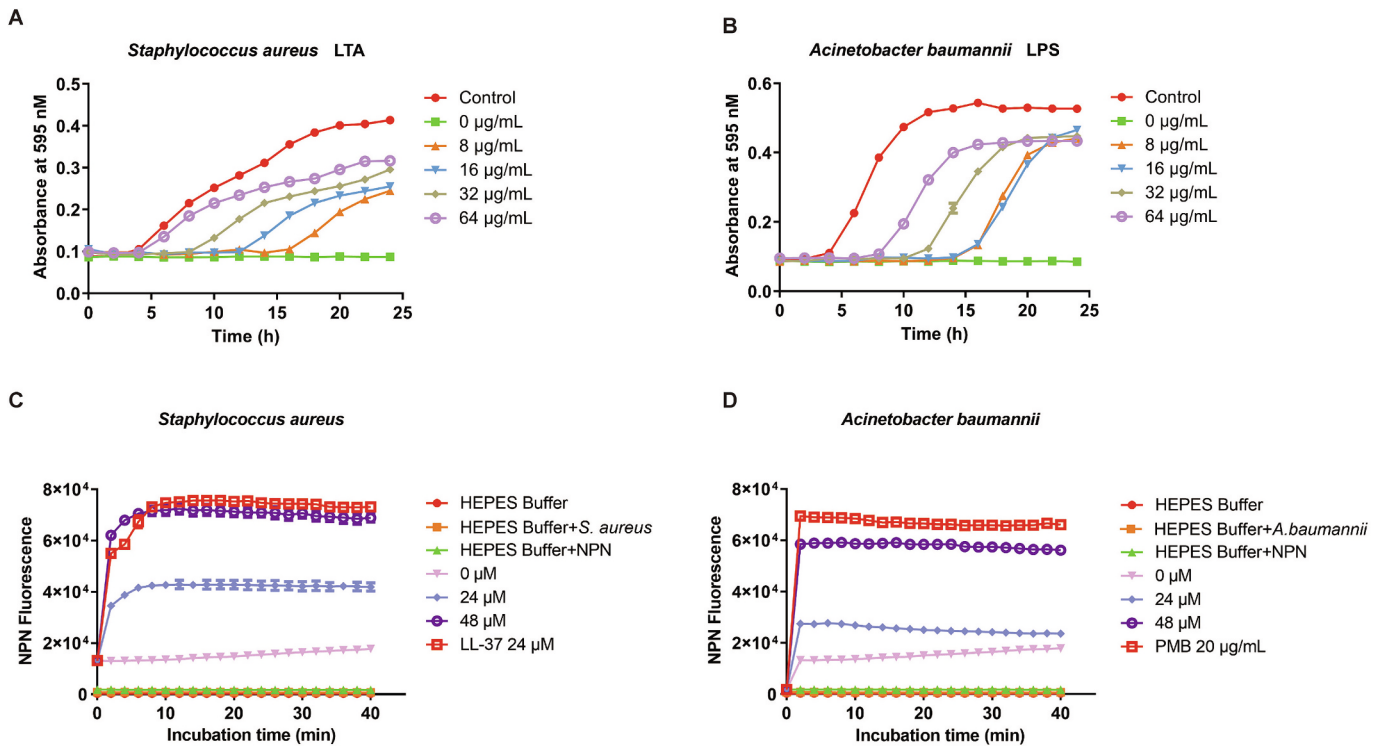


**Fig. 4.** The binding property of Spasin$_{141–165}$ to LTA (A) and LPS (B). The effect of exogenous LPS (0, 8, 16, 32 and 64 μg mL$^{-1}$) on the antibacterial activity of Spasin$_{141–165}$ (1 × MBC) was assessed by measuring the growth curve of *S. aureus*. The effect of exogenous LPS (0, 8, 16, 32, and 64 μg mL$^{-1}$) on the antibacterial activity of Spasin$_{141–165}$ (1 × MBC) was assessed by measuring the growth curve of *A. baumannii*. Bars represent the mean ± standard error of the mean ($n = 3$). (C, D) Outer membrane permeability after Spasin$_{141–165}$ treatment was measured by *N*-phenyl-1-naphthylamine (NPN) uptake assay. NPN fluorescence was recorded at excitation and emission wavelengths of 350 and 420 nm, respectively.

### 3.10. Spasin$_{141–165}$ showed no cytotoxicity

To evaluate the cytotoxicity of Spasin$_{141–165}$, several cell lines were used, including HEK-293 T, RAW 264.7, and ZF4. The results showed that Spasin$_{141–165}$ was not cytotoxic to zebrafish cells and mammalian cells (Fig. 8A & 8C). We further evaluated the hemolytic activity of Spasin$_{141–165}$ on mouse red blood cells. The results showed that Spasin$_{141–165}$ had no hemolytic activity at concentrations ranging from 3 and 48 μM (Fig. 8 D). The results indicated that Spasin$_{141–165}$ had good biocompatibility.

### 3.11. Efficacy of Spasin$_{141–165}$ treatment on A. hydrophila infection in a zebrafish model

We constructed a zebrafish infection model to evaluate the *in vivo* antimicrobial activity of Spasin$_{141–165}$, zebrafish were infected intraperitoneally with *A. hydrophila*, a common aquatic pathogen, and treated with Spasin$_{141–165}$ 1 h after infection (Fig. 9A). The survival rates of Spasin$_{141–165}$-treated and control groups were 70.6% and 50% after 48 h of treatment, respectively. Statistical analysis showed that the survival rate of zebrafish in the Spasin$_{141–165}$ treatment group was significantly higher than that in the control group ($p = 0.0365$) (Fig. 9A). In addition, Spasin$_{141–165}$ treatment significantly reduced the bacterial load in the spleen (Fig. 9B). We further examined the mRNA levels of cytokines in the spleen, and found that several inflammation-associated genes, including IL-1β, MMP9, TNF-α, cxcl8a, and NOS2a, were significantly downregulated in Spasin$_{141–165}$-treated zebrafish. The transcription levels of MMP9 and NOS2a were restored to the same levels as in the controls (Fig. 9C).

## 4. Discussion

A range of bacterial pathogens cause significant losses in aquaculture, accounting for approximately 34% of all diseases (Singh et al., 2022), with *A. hydrophila* being a prevalent aquaculture pathogen that secretes a variety of exotoxins, including aerosols, hemolysins and cytotoxic enterotoxins, upon successful colonization of fish. These toxins can lead to hemolysis and hemorrhage, which reduces the immune response of the host fish, which in turn leads to high host lethality (Gao et al., 2024). Antibiotics are often used in aquaculture to control bacterial diseases in fish, but the use of antibiotics is currently restricted and antibiotic-resistant bacteria strains are on the rise (Singh et al., 2022), and this situation urgently calls for the development of more novel antimicrobial drugs for aquaculture pathogen control.

Crustaceans, including mud crabs, lack adaptive immunity, so their survival depends on strong innate immune anti-infection defense mechanisms (Punginelli et al., 2022; Sperstad et al., 2011). Therefore, they are an important source of numerous naturally occurring bioactive compounds, including AMPs. With broad-spectrum antimicrobial activity and unique modes of action, natural AMPs are receiving increasing attention as potential alternatives to antibiotics (Chen et al., 2021). AMPs are widely distributed in a variety of species in nature (Boman and Hultmark, 1987; Park et al., 2001; Zasloff, 2002), and are important effectors of the innate immune system, with abundant biological activities that serve as the first line of defense against pathogenic infections (Diamond et al., 2009; Méndez-Samperio, 2013; Reddy et al., 2004), as well as modulating the immune system and exerting anti-inflammatory activities (Ahmed and Hammami, 2019; Haney et al., 2019; Wang et al., 2019).

In this study, we screened a novel functional gene named Spasin from the transcriptomics database of *Vibrio alginolyticus*-infected mud crabs. Based on the bioinformatics analysis and validation, we successfully

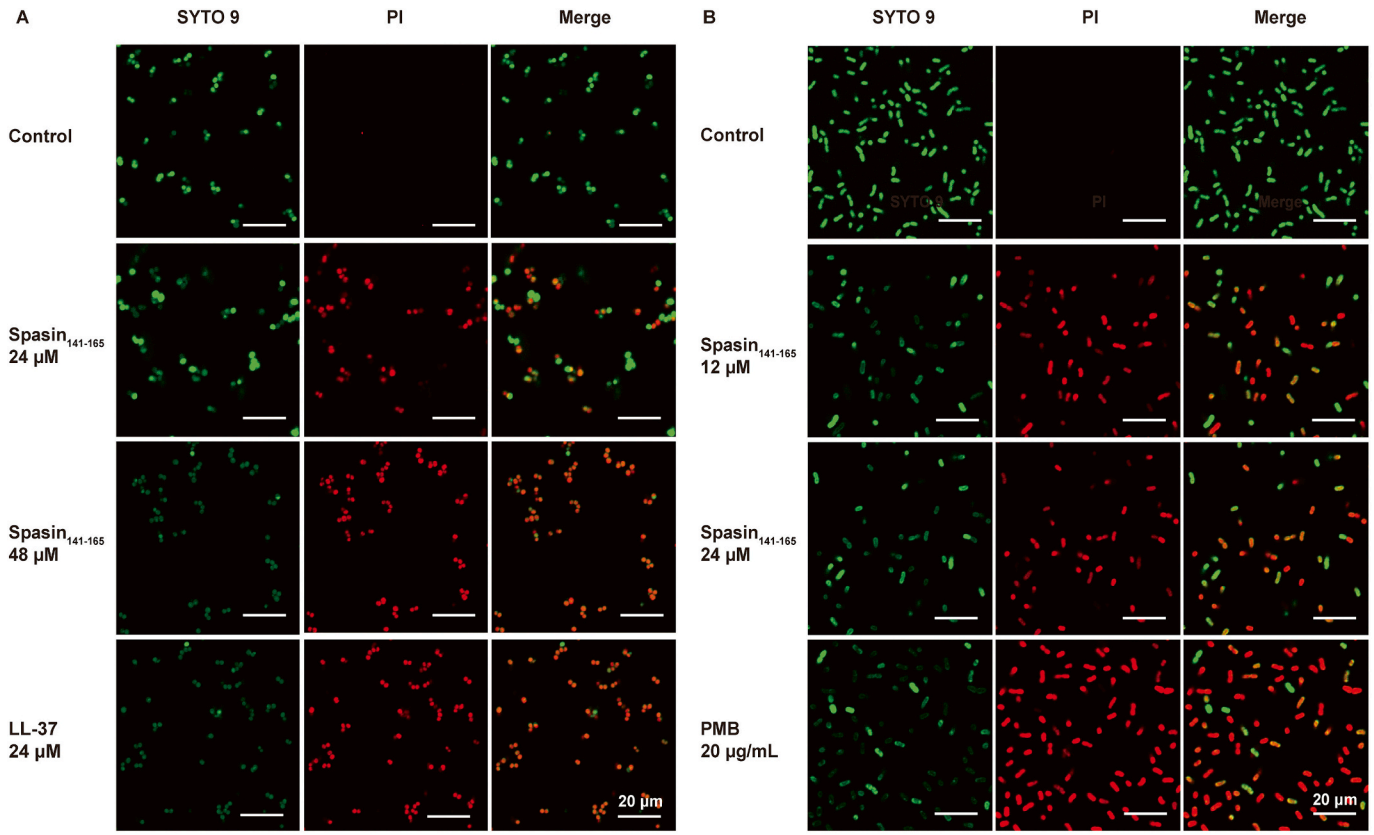


**Fig. 5.** Effect of Spasin$_{141–165}$ on the membrane permeability of *S. aureus* (A) and *A. baumannii* (B). Confocal laser-scanning microscope (CLSM) images showing cell membrane permeability by SYTO 9 and propidium iodide (PI) staining in *S. aureus* and *A. baumannii* cells treated with Spasin$_{141–165}$.

identified a new AMP, which was a truncated peptide Spasin$_{141–165}$ derived from Spasin. We characterized the physicochemical properties and antimicrobial activity of Spasin$_{141–165}$ to elucidate its antimicrobial effect against *A. hydrophila* infections and its intrinsic mechanism, providing new insights into the development of alternatives to antibiotics for future applications in aquaculture. It is now widely accepted that the net charge and length of AMPs are among the most critical parameters for their antimicrobial activity (Islam et al., 2023). Spasin$_{141–165}$ carries a high positive charge number of +7 and has potent broad-spectrum antimicrobial activity against bacteria and fungi. Similar to the binding properties of other cationic AMPs (Islam et al., 2023), the positive charge of spasin$_{141–165}$ might enhance binding to negatively charged microbial surfaces through electrostatic interaction.

We found that, like most AMPs (Huo et al., 2020; Ma et al., 2016), the main antibacterial mechanism of Spasin$_{141–165}$ was the disruption of bacterial membranes, leading to leakage of intracellular content and ultimately leading to bacterial death. In the study, we observed the disruptive effect of Spasin$_{141–165}$ on the morphological structure of bacteria by SEM and TEM, and confirmed the penetration of Spasin$_{141–165}$ into the outer and inner membranes of bacteria by NPN, SYTO9, and PI staining. Spasin$_{141–165}$ was able to act on cell membranes, resulting in the rupture of the cell membrane and surface crumpling. Furthermore, we observed an increase in the level of ATP, a key cellular component, after Spasin$_{141–165}$ treatment, which could be attributed to the damage of the cell membrane and the reduction of the bacterial barrier function, which in turn led to the release of ATP.

In general, both Gram-negative and Gram-positive bacteria contain negatively charged phospholipids, giving the microorganisms a net negative charge on the cell surface (Ma et al., 2016; Xhindoli et al., 2016). In addition, Gram-negative bacteria contain LPS while Gram-positive bacteria contain LTA, both of which are negatively charged substances (Bhattacharya et al., 2018). In fact, the results of the inhibitory effect of the bacterial membrane components LTA and LPS on the antimicrobial activity of Spasin$_{141–165}$ showed that the susceptibility of *S. aureus* or *A. baumannii* to Spasin$_{141–165}$ was reduced by the addition of LTA or LPS, which implies that Spasin$_{141–165}$ might bind to the membrane components of the microorganisms, thereby reducing the ability of the peptide to target cell membranes, and thus diminishing the antimicrobial activity. Similarly, cationic AMPs (*e.g.* Epinecidin-1) can bind to negatively charged components of bacterial cell membranes through electrostatic interactions, thereby accumulating on the bacterial surface and killing the bacteria by lysing the cell membranes after reaching the action concentration (Narayana et al., 2015). In the study, we observed elevated levels of bacterial ROS induced by Spasin$_{141–165}$. ROS can be produced by the electron transport chain of aerobic respiration, which helps to maintain normal physiological activities of bacteria. As reported, during treatment of bacteria with AMPs, large amounts of ROS are produced and accumulated, and excessive ROS will cause oxidative stress, leading to oxidative damage, which in turn affects bacterial activities (He et al., 2021; Lee et al., 2020; Wang et al., 2018). In the study, Spasin$_{141–165}$ treatment effectively altered the permeability of bacterial cell membranes, while inducing excessive and lethal production of ROS.

In order to evaluate whether Spasin$_{141–165}$ has potential applications, we determined that Spasin$_{141–165}$ is affected by various factors (*e.g.*, temperature, cations, *etc.*). The results showed that Spasin$_{141–165}$ has strong thermal stability as its antimicrobial activity against *S. aureus* and *A. baumannii* after 120 min of boiling water treatment. This is similar to the properties of many other AMPs, such as BAMP (Choyam et al., 2021), which has good thermal stability. This means that Spasin$_{141–165}$ can be used in potentially high-temperature environments associated with aquaculture while maintaining good antimicrobial activity.

Cations are often considered a barrier to the antimicrobial activity of AMPs because the electrostatic force between the positive charge carried

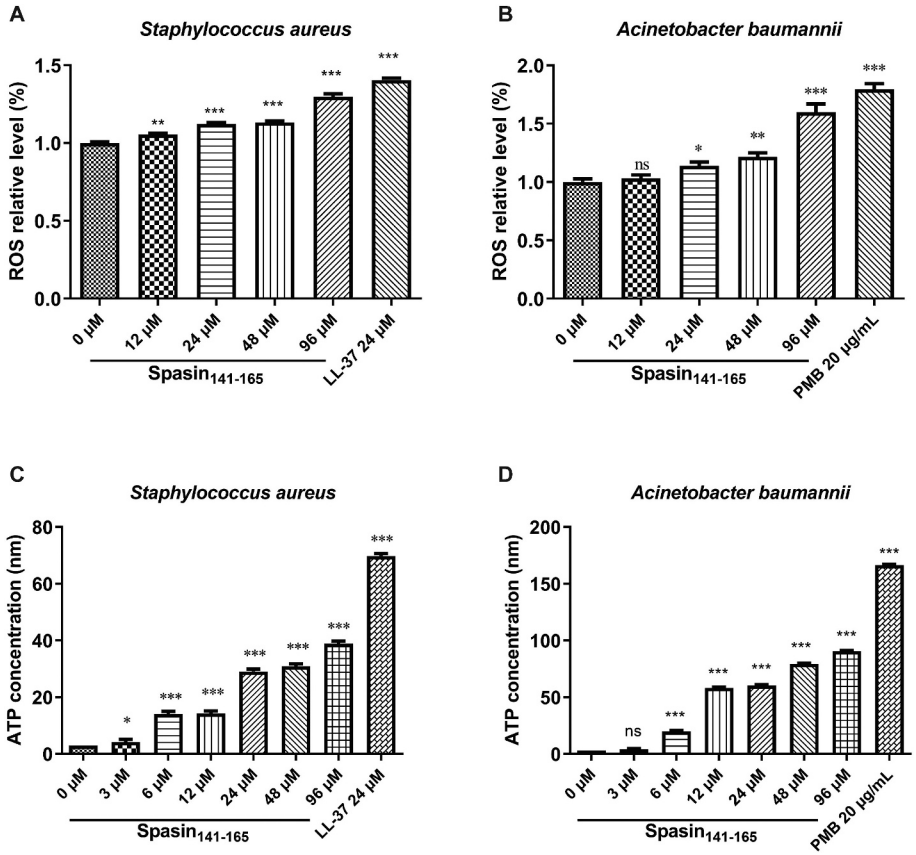


**Fig. 6.** Effect of different concentrations of $Spasin_{141–165}$ on intracellular reactive oxygen species levels (A, B) and on ATP release (C, D). Significant differences were indicated by an asterisk, $*p < 0.05$, $**p < 0.01$, $***p < 0.001$. Bars represent the mean ± standard error of the mean ($n = 3$).

by the AMPs and the negative charge carried by the bacterial surface is easily disrupted in the presence of cations (Xian et al., 2022). We evaluated the ionic tolerance of $Spasin_{141–165}$. The antimicrobial activity of $Spasin_{141–165}$ at the marine environment $K^+$ concentration (2–10 mM), whereas $Na^+$ concentration affected the antimicrobial activity of $Spasin_{141–165}$ to varying degrees. Interestingly, the antimicrobial activity of $Spasin_{141–165}$ against *S. aureus* was unaffected at 100 mM $Na^+$, whereas the antimicrobial activity of $Spasin_{141–165}$ against *A. baumannii* was inhibited under the same conditions. It has been reported that divalent cations may reduce the antimicrobial activity of AMPs, such as LL-37 (Bowdish et al., 2005) and human β-defense-1 (Goldman et al., 1997).

A major obstacle to the use of AMPs as alternatives to conventional antibiotics is their potential cytotoxicity. Most α-helical AMPs are not selective for microbial cells and exhibit toxicity to animal cells (Luo et al., 2021; Soman et al., 2009). We evaluated the cytotoxicity and hemolytic activity of $Spasin_{141–165}$. The results showed that $Spasin_{141–165}$ was non-toxic to human embryonic kidney cells (HEK-293 T), mouse macrophages (RAW 264.7), and zebrafish embryonic fibroblasts (ZF4) and had no hemolytic activity on mouse erythrocytes, implying that it has good biocompatibility. It has been reported that AMPs with a net charge higher than +6 may lead to increased toxicity (Oren and Shai, 1998), whereas $Spasin_{141–165}$ with a total net charge of +7 still showed no significant cytotoxicity. In contrast, LL-37 with a total net charge of +6 showed higher cytotoxicity and hemolytic activity (Tan et al., 2021; Yeaman and Yount, 2005). $Spasin_{141–165}$ has strong antibacterial activity against free-living planktonic bacteria *in vitro*, but its antibacterial activity against biofilm-associated bacteria is unknown. It is generally believed that biofilm-associated bacteria are less sensitive to antimicrobial agents than free-living planktonic cells (Acosta et al., 2021), and the anti-bacterial biofilm activity and mechanism of $Spasin_{141–165}$ deserve further investigation.

Finally, we investigated whether $Spasin_{141–165}$ has an *in vivo* anti-infective effect by modeling bacterial infection in zebrafish. Although $Spasin_{141–165}$ had no inhibitory effect on *A. hydrophila in vitro*, treatment of $Spasin_{141–165}$ after bacterial infection significantly increased the survival rate of zebrafish, suggesting that $Spasin_{141–165}$ has potential as an antibacterial agent. Inflammation was induced in zebrafish infected with *A. hydrophila* through innate immune response, and a large number of immune cells infiltrate the site of inflammation and release inflammatory factors, such as TNF-α, IL-1β, cxcl8a, *etc.*, which leads to a dysregulation of the immune homeostasis (Liu et al., 2014; Rosales and Uribe-Querol, 2017). Immune cells and immune factors play an important role in the development of inflammatory responses, and IL-1β is an important signal for early immune responses and a key mediator of microbial invasion (Liu et al., 2014). As reported, it was found that IL-1β was significantly up-regulated in zebrafish spleen after intraperitoneal injection of *Edwardsiella tarda* (Mohanty and Sahoo, 2010; Pressley et al., 2005). In our study, IL-1β was significantly upregulated in *A. hydrophila*-infected zebrafish spleens, suggesting that the early inflammatory immune response was stimulated after infection. As one of the pro-inflammatory factors, IL-1β activates immune cells that stimulate and secrete pro-inflammatory cytokines, creating a positive feedback regulatory loop (Hiroko et al., 2015). Another cytokine, TNF-α, promotes the expression of *E*-selectin as well as different CC and CXC chemokines in endothelial cells, thus contributing to phagocyte recruitment and activation, and bacterial infections are capable of inducing TNF-α production by macrophages in fish (Ishibe et al., 2009; Roca et al., 2008). We found that treatment with $Spasin_{141–165}$ reduced the transcription levels of IL-1β and TNF-α, and attenuated the inflammatory immune response, while the transcriptional expression levels of the neutrophil chemokine cxcl8 were inhibited. It is noting that NOS2a

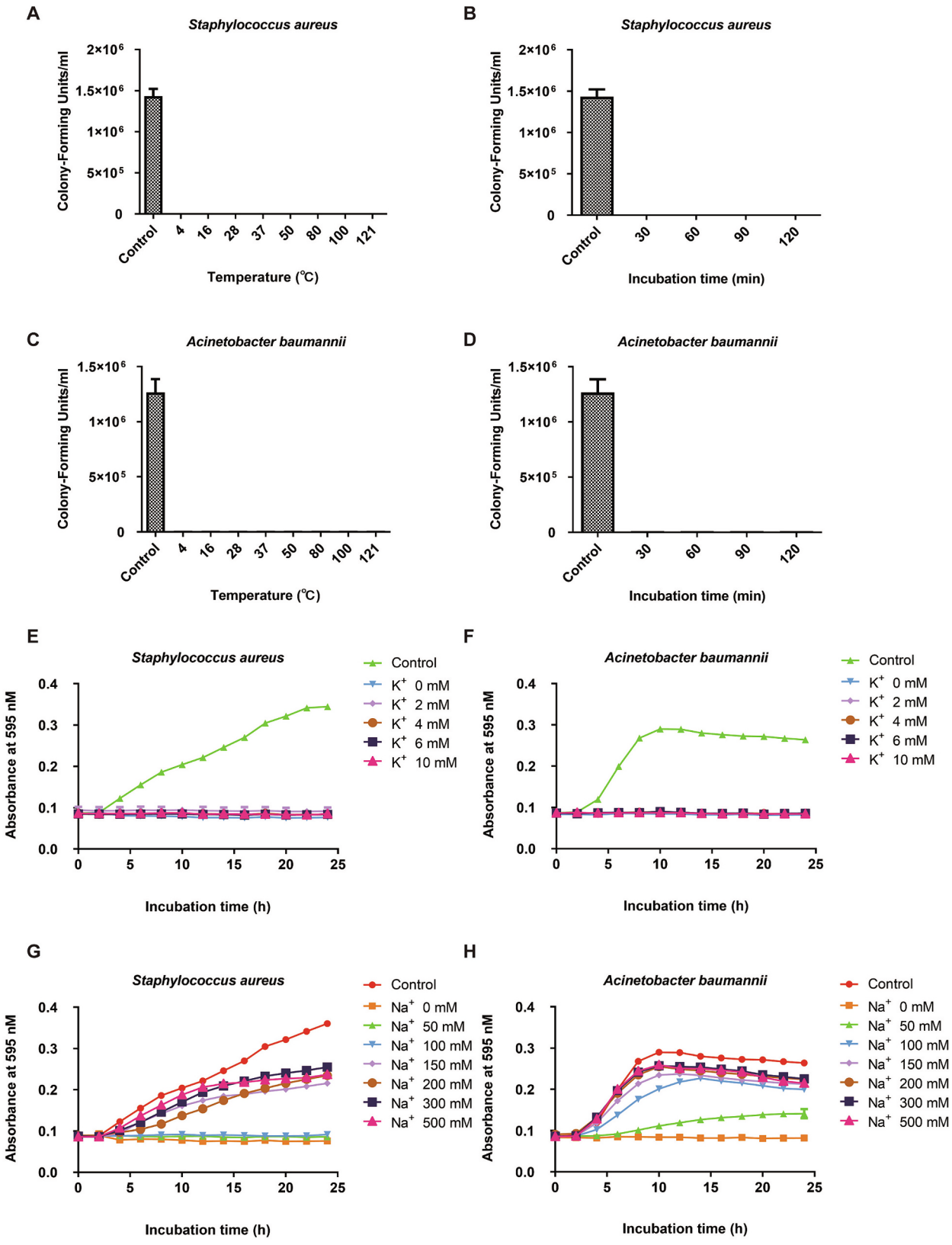


**Fig. 7.** Thermal stability of Spasin$_{141–165}$. *S. aureus* and *A. baumannii* were treated with heated Spasin$_{141–165}$ at a concentration of 1 × MBC (A-D). Bacteria treated without Spasin$_{141–165}$ were used as control groups. Effect of different cation concentration conditions on the sensitivity of bacteria to Spasin$_{141–165}$ (*E*-H). The antimicrobial activity of Spasin$_{141–165}$ against *S. aureus* (E) and *A. baumannii* (F) under various concentrations of KCl. The antimicrobial activity of Spasin$_{141–165}$ against *S. aureus* (G) and *A. baumannii* (H) under various concentrations of NaCl.

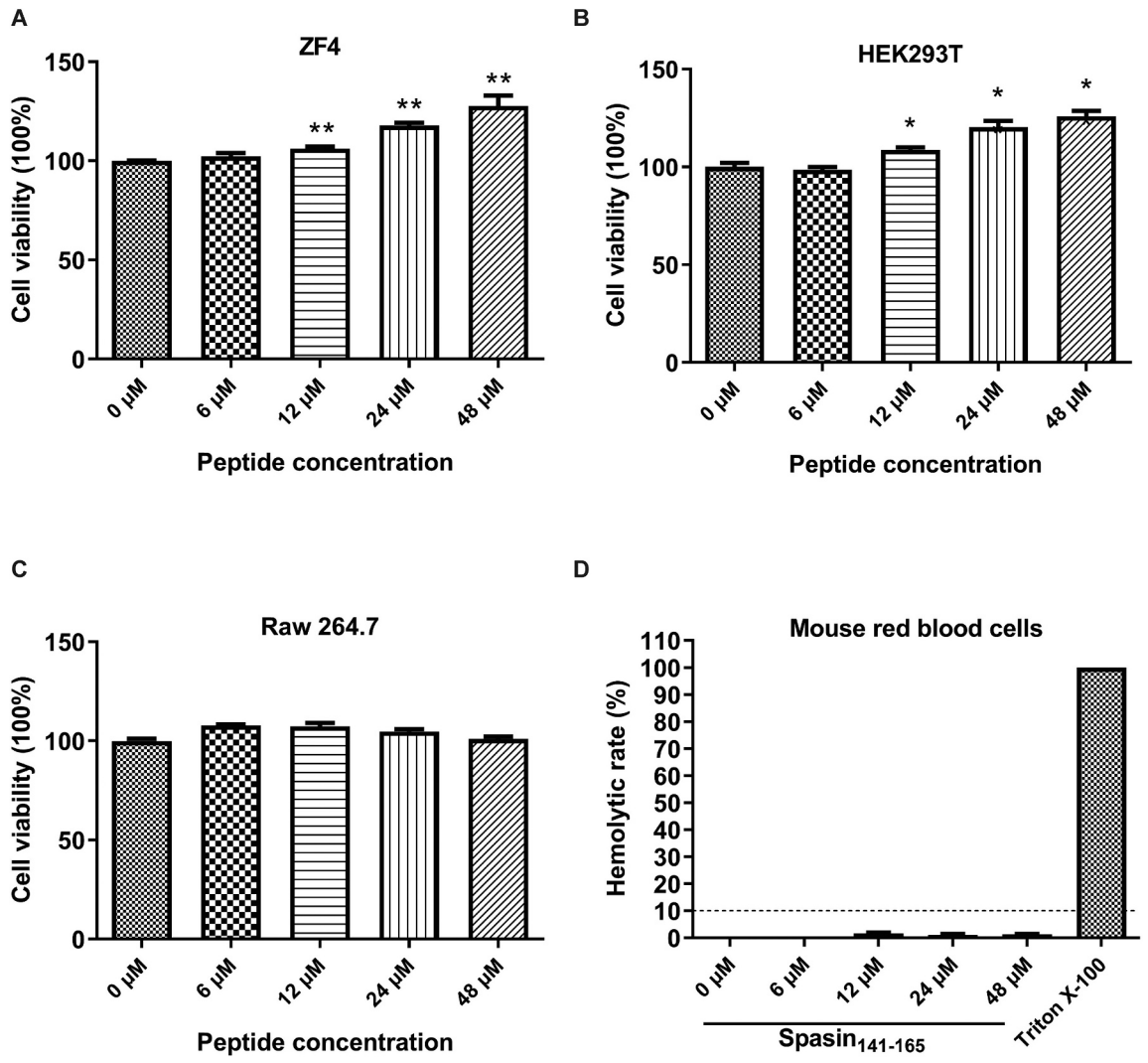


**Fig. 8.** *In vitro* cytotoxicity and hemolytic activity. The cytotoxicity of $Spasin_{141–165}$ on zebrafish embryonic fibroblasts (ZF4) (A), human embryonic kidney cells (HEK-293 T) (B), and mouse macrophages (RAW 264.7) (C) was determined by the MTS-PMS assay. Hemolytic activity of $Spasin_{141–165}$ against mouse red blood cells (D). The significant difference between the control group and the $Spasin_{141–165}$ treatment group was indicated by asterisks as $^{*}p < 0.05$, $^{**}p < 0.01$, $^{***}p < 0.001$. Bars indicate the mean ± standard error of the mean ($n = 3$). (For interpretation of the references to colour in this figure legend, the reader is referred to the web version of this article.)

is expressed mainly in immune tissues (*e.g.*, spleen) and pathogen-invasive organs (*e.g.*, gills, skin, and intestine), and is to some extent a feature of pathogenic infections (Nath and Maitra, 2019), and interestingly, $Spasin_{141–165}$ reversed the transcription levels of NOS2a. In addition, MMP9 is an inflammatory mediator involved in the development of many diseases, such as inflammatory response (Falardeau et al., 2001). We found that $Spasin_{141–165}$ reduced the transcripts of MMP9 to levels comparable to those of controls. Taken together, these results indicated that $Spasin_{141–165}$ could effectively control *A. hydrophila* infection in zebrafish, significantly increase the survival rate of zebrafish, and effectively reduce the inflammatory response of zebrafish after infection. In a follow-up study, several representative freshwater edible fish (such as grass carp (*Ctenopharyngodon idella*), freshwater eel (*Anguilla japonica*) and silver carp (*Hypophthalmichthys molitrix*)) will be selected to further evaluate the *in vivo* anti-*A. hydrophila* infection effect of $Spasin_{141–165}$. We believe that this study will provide new ideas for the control of *A. hydrophila* infections in aquaculture, and $Spasin_{141–165}$ has the potential to become a safe and effective new antimicrobial agent.

## 5. Conclusions

In conclusion, we identified a novel functional gene named Sapsin in mud crabs. Based on the prediction and analysis of Spasin, we identified a novel AMP, $Spasin_{141–165}$, with broad-spectrum antimicrobial activity. $Spasin_{141–165}$ disrupted the cell membranes of *S. aureus* and *A. baumannii*, increased membrane permeability, induced the accumulation of ROS and the release of ATP, and finally killed the bacteria. $Spasin_{141–165}$ had good biocompatible and was non-cytotoxic to mammalian and zebrafish cells. Notably, $Spasin_{141–165}$ treatment significantly enhanced the survival of zebrafish infected with *A. hydrophila*, reduced the bacterial load in spleen and suppressed the expression of several inflammation-associated genes. The discovery and identification of $Spasin_{141–165}$ will add to the list of marine-derived AMPs that could be used as drug candidates against microbial infections in the future.

## CRediT authorship contribution statement

**Chang Zhang:** Writing – original draft, Methodology, Investigation, Formal analysis, Data curation. **Fangyi Chen:** Writing – review &

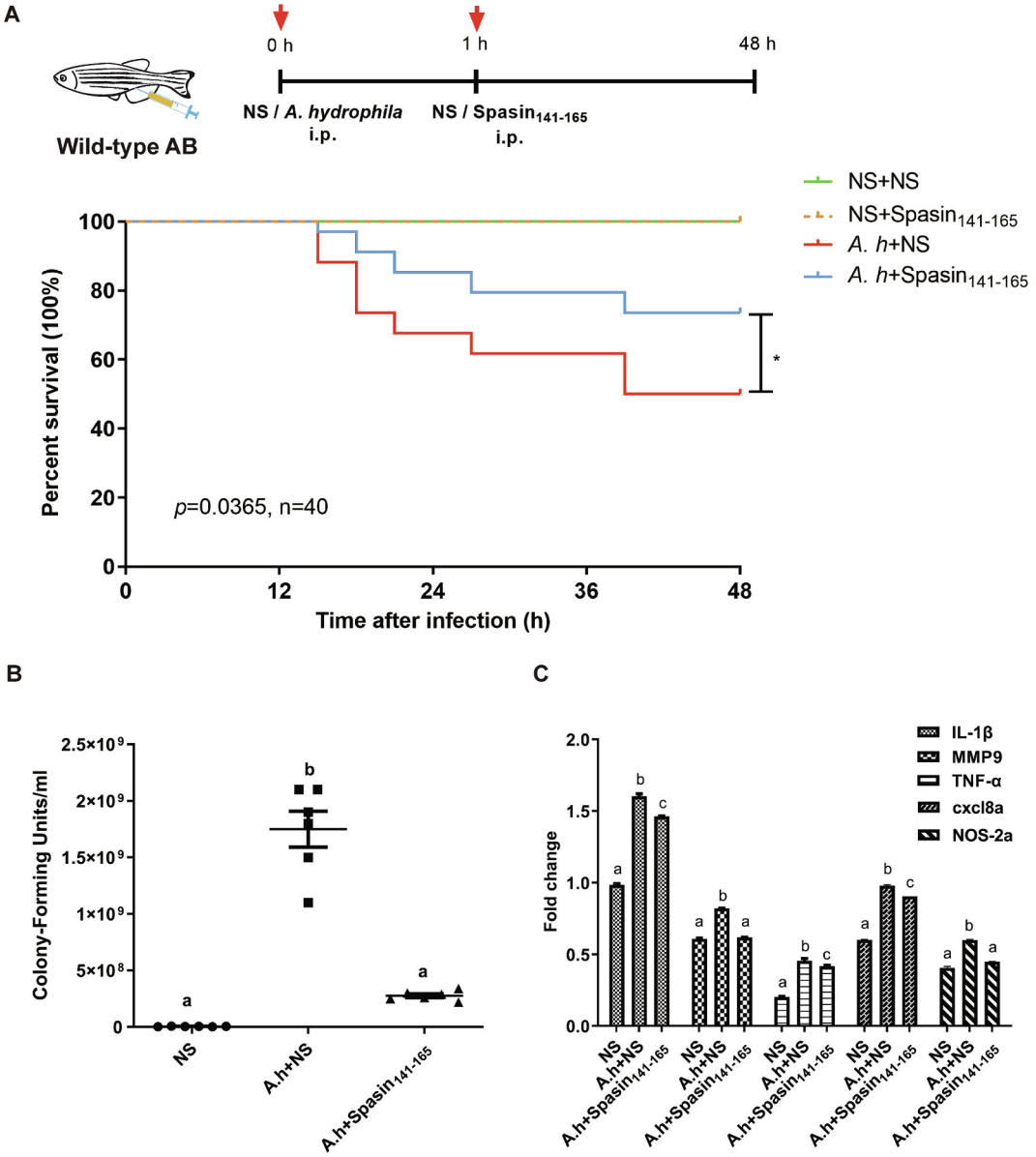


**Fig. 9.** The effectiveness of Spasin$_{141–165}$ in *A. hydrophila* infected zebrafish. Scheme of bacterial infection in zebrafish and the survival curve was analyzed using the Kaplan-Meier log-rank test ($n = 40$) (A). Bacterial load in zebrafish spleen ($n = 5$) (B). Expression of inflammation-related genes in the zebrafish spleen ($n = 5$) (C),. $^{*}p < 0.05$, $^{**}p < 0.01$, $^{***}p < 0.001$ indicated significant differences.

editing, Supervision, Project administration, Funding acquisition, Conceptualization. **Yuqi Bai:** Methodology, Investigation. **Xianxian Dong:** Methodology, Investigation. **Xinzhan Meng:** Methodology, Investigation. **Ke-Jian Wang:** Writing – review & editing, Supervision, Project administration, Funding acquisition, Conceptualization.

## Declaration of competing interest

The authors declare that the research was conducted in the absence of any commercial or financial relationships that could be construed as a potential conflict of interest.

## Data availability

No data was used for the research described in the article.

## Acknowledgments

This work was supported by the National Natural Science Foundation of China with grant number (42376089/U1805233/41806162); the Natural Science Foundation of Fujian Province, China with grant number with grant number (2021J05008); Fujian Ocean and Fisheries Bureau with grant number (FJHY-YYKJ-2022-1-14); Fujian Ocean Synergy Alliance with grant number (FOCAL2023-0207), Xiamen Ocean Development Bureau with grant number (22CZP002HJ08), and Pingtan Research Institute of Xiamen University with grant number (Z20220743). We thank laboratory engineers Hui Peng, Huiyun Chen, Zhiyong Lin, Hua Hao and Ming Xiong for providing technical assistance.

## Appendix A. Supplementary data

Supplementary data to this article can be found online at https://doi.org/10.1016/j.aquaculture.2024.741137.

## References


Acosta, F., Montero, D., Izquierdo, M., Galindo-Villegas, J., 2021. High-level biocidal products effectively eradicate pathogenic γ-proteobacteria biofilms from aquaculture facilities. Aquaculture. 532, 736004.

Ahmed, T.A.E., Hammami, R., 2019. Recent insights into structure-function relationships of antimicrobial peptides. J. Food Biochem. 43 (1), e12546.

Bhattacharya, G., Giri, R.P., Dubey, A., Mitra, S., Priyadarshini, R., Gupta, A., Mukhopadhyay, M.K., Ghosh, S.K.J.C., Lipids, P.o., 2018. Structural changes in cellular membranes induced by ionic liquids: from model to bacterial membranes. Chem. Phys. Lipids 215, 1–10.

Boman, H.G., Hultmark, D., 1987. Cell-free immunity in insects. Annu. Rev. Microbiol. 41, 103–126.

Bowdish, D.M.E., Davidson, D.J., Lau, Y.E., Lee, K., Scott, M.G., Hancock, R.E.W., 2005. Impact of LL- 37 on anti-infective immunity. J. Leukoc. Biol. 77 (4), 451–459.

Browne, A.J., Chipeta, M.G., Haines-Woodhouse, G., Kumaran, E.P.A., Hamadani, B.H. K., Zaraa, S., Henry, N.J., Deshpande, A., Reiner Jr., R.C., Day, N.P.J., Lopez, A.D., Dunachie, S., Moore, C.E., Stergachis, A., Hay, S.I., Dolecek, C., 2021. Global antibiotic consumption and usage in humans, 2000-18: a spatial modelling study. Lancet Planet Health. 5 (12), e893–e904.

Bungau, S., Tit, D.M., Behl, T., Aleya, L., Zaha, D.C., 2021. Aspects of excessive antibiotic consumption and environmental influences correlated with the occurrence of resistance to antimicrobial agents. Curr. Environ. Health Rep. 19 (2020).

Chen, F., Wang, K., 2019. Characterization of the innate immunity in the mud crab *Scylla paramamosain*. Fish Shellfish Immun. 93, 436–448.

Chen, Y.C., Yang, Y., Zhang, C., Chen, H.Y., Chen, F., Wang, K.J., 2021. A novel antimicrobial peptide sparamosin$_{26\text{-}54}$ from the mud crab *Scylla paramamosain* showing potent antifungal activity against *Cryptococcus neoformans*. Front. Microbiol. 12, 746006.

Choyam, S., Jain, P.M., Kammara, R.J., 2021. Characterization of a potent new-generation antimicrobial peptide of *Bacillus*. Front. Microbiol. 12, 2236.

Ciumac, D., Gong, H., Hu, X., Lu, J.R., 2019. Membrane targeting cationic antimicrobial peptides. J. Colloid Interface Sci. 537, 163–185.

Claudiano, G.S., Yunis-Aguinaga, J., Marinho-Neto, F.A., Miranda, R.L., Martins, I.M., Otani, F.S., Mundim, A.V., Marzocchi-Machado, C.M., Moraes, J.R.E., de Moraes, F. R., 2019. Hematological and immune changes in *Piaractus mesopotamicus* in the sepsis induced by *Aeromonas hydrophila*. Fish Shellfish Immun. 88, 259–265.

Corrêa, J.A.F., Evangelista, A.G., Nazareth, T.d.M., Luciano, F.B., 2019. Fundamentals on the molecular mechanism of action of antimicrobial peptides. Materialia. 8.

Correia, S., Poeta, P., Hébraud, M., Capelo, J.L., Igrejas, G., 2017. Mechanisms of quinolone action and resistance: where do we stand? J. Med. Microbiol. 66 (5), 551–559.

Daood, N., 2012. Isolation and Antibiotic Susceptibility of *Aeromonas* spp. from Freshwater Fish Farm and Farmed Farp (Dam of 16 Tishreen Lattakia).

De Santis, E., Alkassem, H., Lamarre, B., Faruqui, N., Bella, A., Noble, J.E., Micale, N., Ray, S., Burns, J.R., Yon, A.R., Hoogenboom, B.W., Ryadnov, M.G., 2017. Antimicrobial peptide capsids of de novo design. Nat. Commun. 8 (1), 2263.

Deo, S., Turton, K.L., Kainth, T., Kumar, A., Wieden, H.-J., 2022. Strategies for improving antimicrobial peptide production. Biotechnol. Adv. 59, 107968.

Diamond, G., Beckloff, N., Weinberg, A., Kisich, K.O., 2009. The roles of antimicrobial peptides in innate host defense. Curr. Pharm. Design. 15 (21), 2377–2392.

Ding, D., Wang, B., Zhang, X., Zhang, J., Zhang, H., Liu, X., Gao, Z., Yu, Z., 2023. The spread of antibiotic resistance to humans and potential protection strategies. Ecotox. Environ. Safe. 254, 114734.

Falardeau, P., Champagne, P., Poyet, P., Hariton, C., Dupont, É., 2001. Neovastat, a naturally occurring multifunctional antiangiogenic drug, in phase III clinical trials. Semin. Oncol. 28 (6), 620–625.

Gao, J.-h., Zhao, J.-l., Yao, X.-l., Tola, T., Zheng, J., Xue, W.-b., Wang, D.-w., Xing, Y., 2024. Identification of antimicrobial peptide genes from transcriptomes in Mandarin fish (*Siniperca chuatsi*) and their response to infection with *Aeromonas hydrophila*. Fish Shellfish Immun. 144, 109247.

Goldman, Mitchell J., Anderson, G., Mark, Stolzenberg, Ethan, D., Cell, K.J., 1997. Human beta-defensin-1 is a salt-sensitive antibiotic in lung that is inactivated in cystic fibrosis. CELL. 88 (4), 553–560.

Greber, K.E., Roch, M., Rosato, M.A., Martinez, M.P., Rosato, A.E., 2020. Efficacy of newly generated short antimicrobial cationic lipopeptides against methicillin-resistant *Staphylococcus aureus* (MRSA). Int. J. Antimicrob. Agents 55 (3), 105827.

Haney, E.F., Straus, S.K., Hancock, R.E.W., 2019. Reassessing the host defense peptide landscape. Front. Chem. 7, 43.

He, Z., Xu, Q., Newland, B., Foley, R., Curtin, J.F., Wang, W., 2021. Reactive oxygen species (ROS): utilizing injectable antioxidative hydrogels and ROS-producing therapies to manage the double-edged sword. J. Mater. Chem. B 9 (32), 6326–6346.

Hiroko, T., Xianbin, C., Shuhei, H.J., 2015. Interleukin-1 family cytokines in liver diseases. Mediat. Inflamm. 2015, 1–19.

Hu, Y., Cheng, H., 2016. Health risk from veterinary antimicrobial use in China's food animal production and its reduction. Environ. Pollut. 219, 993–997.

Hu, Y., Gao, G.F., Zhu, B., 2017. The antibiotic resistome: gene flow in environments, animals and human beings. Front. Med. 11 (2), 161–168.

Huo, S., Chen, C., Lyu, Z., Zhang, S., Yue, B.J.., 2020. Overcoming planktonic and intracellular *staphylococcus aureus* -associated infection with a cell-penetrating peptide-conjugated antimicrobial peptide. Acs Infect Dis. 6 (12), 3147–3162.

Igbinosa, I.H., Igumbor, E.U., Aghdasi, F., Tom, M., Okoh, A.I., 2012. Emerging *Aeromonas* species infections and their significance in public health. ScientificWorld J. 2012, 625023.

Ishibe, K., Yamanishi, T., Wang, Y., Osatomi, K., Hara, K., Kanai, K., Yamaguchi, K., Oda, T., 2009. Comparative analysis of the production of nitric oxide (NO) and tumor necrosis factor-α (TNF-α) from macrophages exposed to high virulent and low virulent strains of *Edwardsiella tarda*. Fish Shellfish Immun. 27 (2), 386–389.

Islam, M.M., Asif, F., Zaman, S.U., Arnab, M.K.H., Rahman, M.M., Hasan, M., 2023. Effect of charge on the antimicrobial activity of alpha-helical amphibian antimicrobial peptide. Curr. Res. Microbial Sci. 4.

Ji, S., An, F., Zhang, T., Lou, M., Guo, J., Liu, K., Zhu, Y., Wu, J., Wu, R., 2024. Antimicrobial peptides: An alternative to traditional antibiotics. Eur. J. Med. Chem. 5 (265), 116072.

Jiang, M., Chen, R., Zhang, J., Chen, F., Wang, K.J., 2022. A novel antimicrobial peptide spampcin$_{56\text{-}86}$ from *Scylla paramamosain* exerting rapid bactericidal and anti-biofilm activity *in vitro* and anti-infection *in vivo*. Int. J. Mol. Sci. 23 (21).

Lee, B., Hwang, J.S., Lee, D.G., 2020. Antibacterial action of lactoferricin B like peptide against *Escherichia coli*: reactive oxygen species-induced apoptosis-like death. J. Appl. Microbiol. 129 (2), 287–295.

Liu, X., Chang, X., Wu, H., Xiao, J., Gao, Y., Zhang, Y., 2014. Role of intestinal inflammation in predisposition of *Edwardsiella tarda* infection in zebrafish (*Danio rerio*). Fish Shellfish Immun. 41 (2), 271–278.

Liu, X., Sun, W., Zhang, Y., Zhou, Y., Xu, J., Gao, X., Zhang, S., Zhang, X., 2020. Impact of *Aeromonas hydrophila* and infectious spleen and kidney necrosis virus infections on susceptibility and host immune response in Chinese perch (*Siniperca chuatsi*). Fish Shellfish Immun. 105, 117–125.

Livak, K.J., Schmittgen, T.D., 2001. Analysis of relative gene expression data using real-time quantitative pcr and the $2^{-\Delta\Delta C\hat{T}}$ method. Methods. 25 (4), 402–408.

Luo, X., Ye, X., Ding, L., Zhu, W., Zhao, Z., Luo, D., Liu, N., Sun, L., Chen, Z., 2021. Identification of the scorpion venom-derived antimicrobial peptide Hp1404 as a new antimicrobial agent against carbapenem-resistant *Acinetobacter baumannii*. Microb. Pathog. 157, 104960.

Ma, L., Wang, Y., Wang, M., Tian, Y., Kang, W., Liu, H., Wang, H., Dou, J., Zhou, C., 2016. Effective antimicrobial activity of Cbf-14, derived from a cathelin-like domain, against penicillin-resistant bacteria. Biomaterials. 87, 32–45.

Malekkhaiat Häffner, S., Malmsten, M., 2018. Influence of self-assembly on the performance of antimicrobial peptides. Curr. Opin. Colloid In. 38, 56–79.

Méndez-Samperio, P., 2013. Recent advances in the field of antimicrobial peptides in inflammatory diseases. Adv. Biomed. Res. 2, 50.

Mohanty, B.R., Sahoo, P.K., 2010. Immune responses and expression profiles of some immune-related genes in Indian major carp, *Labeo rohita* to *Edwardsiella tarda* infection. Fish Shellfish Immun. 28 (4), 613–621.

Narayana, J.L., Huang, H.N., Wu, C.J., Chen, J.Y., 2015. Epinecidin-1 antimicrobial activity: *in vitro* membrane lysis and *in vivo* efficacy against *Helicobacter pylori* infection in a mouse model. Biomaterials. 61, 41–51.

Nath, P., Maitra, S., 2019. Physiological relevance of nitric oxide in ovarian functions: an overview. Gen. Comp. Endocrinol. 279, 35–44.

Nordstrom, R., Nystrom, L., Andren, O.C.J., Malkoch, M., Umerska, A., Davoudi, M., Schmidtchen, A., Malmsten, M., 2018. Membrane interactions of microgels as carriers of antimicrobial peptides. J. Colloid Interface Sci. 513, 141–150.

Oliveira, J.T.A., Souza, P.F.N., Vasconcelos, I.M., Dias, L.P., Martins, T.F., Van Tilburg, M.F., Guedes, M.I.F., Sousa, D.O.B., 2019. Mo-CBP3-PepI, Mo-CBP3-PepII, and Mo-CBP3-PepIII are synthetic antimicrobial peptides active against human pathogens by stimulating ROS generation and increasing plasma membrane permeability. Biochimie. 157, 10–21.

Oren, Z., Shai, Y., 1998. Mode of action of linear amphipathic alpha-helical antimicrobial peptides. Biopolymers. 6, 47.

Park, S., Park, S.H., Ahn, H.C., Kim, S., Kim, S.S., Lee, B.J., Lee, B.J., 2001. Structural study of novel antimicrobial peptides, nigrocins, isolated from *Rana nigromaculata*. FEBS Lett. 507 (1), 95–100.

Pressley, M.E., Phelan, P.E., Eckhard Witten, P., Mellon, M.T., Kim, C.H., 2005. Pathogenesis and inflammatory response to *Edwardsiella tarda* infection in the zebrafish. Dev. Comp. Immunol. 29 (6), 501–513.

Punginelli, D., Schillaci, D., Mauro, M., Deidun, A., Barone, G., Arizza, V., Vazzana, M., 2022. The potential of antimicrobial peptides isolated from freshwater crayfish species in new drug development. Dev. Comp. Immunol. 126, 104258.

Rahman, T., Akanda, M., Rahman, M.M., Chowdhury, 2010. Evaluation of the efficacies of selected antibiotics and medicinal plants on common bacterial fish pathogens. Journal of the Bangladesh Agricultural University 7 (1), 163–168.

Reddy, K.V., Yedery, R.D., Aranha, C., 2004. Antimicrobial peptides: premises and promises. Int. J. Antimicrob. Aging 24 (6), 536–547.

Rhodes, G., Huys, G., Swings, J., McGann, P., Hiney, M., Smith, P., Pickup, R.W., 2000. Distribution of oxytetracycline resistance plasmids between aeromonads in hospital and aquaculture environments: implication of Tn*1721* in dissemination of the tetracycline resistance determinant tet A. Appl. Environ. Microbiol. 66 (9), 3883–3890.

Roca, F.J., Mulero, I., López-Muñoz, A., Sepulcre, M.P., Renshaw, S.A., Meseguer, J., Mulero, V., 2008. Evolution of the inflammatory response in vertebrates: fish TNF-alpha is a powerful activator of endothelial cells but hardly activates phagocytes. J. Immunol. 181 (7), 5071–5081.

Rosales, C., Uribe-Querol, E., 2017. Phagocytosis: a fundamental process in immunity. Biomed. Res. Int. 2017, 9042851.

Semwal, A., Kumar, A., Kumar, N., 2023. A review on pathogenicity of *Aeromonas hydrophila* and their mitigation through medicinal herbs in aquaculture. Heliyon. 9 (3), e14088.

Shan, Z., Zhu, K., Peng, H., Chen, B., Liu, J., Chen, F., Ma, X., Wang, S., Qiao, K., Wang, K., 2016. The new antimicrobial peptide SpHyastatin from the mud crab *Scylla paramamosain* with multiple antimicrobial mechanisms and high effect on bacterial infection. Front. Microbiol. 7, 1140.

Singh, S.K., Meitei, M.M., Choudhary, T.G., Soibam, N., Biswas, P., Waikhom, G., 2022. Chapter 15 - Bacterial diseases in cultured fishes: an update of advances in control measures. In: Bacterial Fish Diseases. Academic Press, pp. 307–335.

Soman, N.R., Baldwin, S.L., Hu, G., Marsh, J.N., Lanza, G.M., Heuser, J.E., Arbeit, J.M., Wickline, S.A., Schlesinger, P.H., 2009. Molecularly targeted nanocarriers deliver the cytolytic peptide melittin specifically to tumor cells in mice, reducing tumor growth. J. Clin. Invest. 119 (9), 2830–2842.

Sperstad, S.V., Haug, T., Blencke, H.M., Styrvold, O.B., Li, C., Stensvag, K., 2011. Antimicrobial peptides from marine invertebrates: challenges and perspectives in marine antimicrobial peptide discovery. Biotechnol. Adv. 29 (5), 519–530.

Stratev, D., Odeyemi, O.A., 2016. Antimicrobial resistance of *Aeromonas hydrophila* isolated from different food sources: a mini-review. J. Infect. Public Heal. 9 (5), 535–544.

Tan, P., Fu, H., Ma, X.J.N.T., 2021. Design, optimization, and nanotechnology of antimicrobial peptides: from exploration to applications. Nano Today 39, 101229.

Tartor, Y.H., El-Naenaeey, E.-S.Y., Abdallah, H.M., Samir, M., Yassen, M.M., Abdelwahab, A.M., 2021. Virulotyping and genetic diversity of *Aeromonas hydrophila* isolated from Nile tilapia (*Oreochromis niloticus*) in aquaculture farms in Egypt. AQUACULTURE. 541, 736781.

Wang, Cheng, Zhao, Gaomei, Song, Chen, Yin, Gong, Yali, Agents, S.J.A. Chemotherapy, 2018. A simplified derivative of human Defensin 5 with potent and efficient activity against multidrug-resistant *Acinetobacter baumannii*. Antimicrob Agents Chem. 62 (2).

Wang, J., Dou, X., Song, J., Lyu, Y., Zhu, X., Xu, L., Li, W., Shan, A., 2019. Antimicrobial peptides: promising alternatives in the post feeding antibiotic era. Med. Res. Rev. 39 (3), 831–859.

Wang, X., Hong, X., Chen, F., Wang, K.J., 2022. A truncated peptide Spgillcin$_{177\text{-}189}$ derived from mud crab *Scylla paramamosain* exerting multiple antibacterial activities. Front. Cell Infect. Microbiol. 12, 928220.

Wang, Dan, Fanxiu, Wu, et al., 2023. China Fisheries Statistical Yearbook. China Agricultural Publishing House.

Whelan, J.A., Russell, N.B., Whelan, M.A., 2003. A method for the absolute quantification of cDNA using real-time PCR. J. Immunol. Methods 278 (1), 261–269.

Xhindoli, D., Pacor, S., Benincasa, M., Scocchi, M., Gennaro, R., Tossi, A., 2016. The human cathelicidin LL-37–A pore-forming antibacterial peptide and host-cell modulator. BBA-Biomembranes. 1858 (3), 546–566.

Xian, W., Hennefarth, M.R., Lee, M.W., Do, T., Lee, E.Y., Alexandrova, A.N., Wong, G.C., 2022. Histidine-mediated ion specific effects enable salt tolerance of a pore-forming marine antimicrobial peptide. Angew. Chem. Int. Edit. 61 (25), e202108501.

Xiong, N.-X., Ou, J., Fan, L.-F., Kuang, X.-Y., Fang, Z.-X., Luo, S.-W., Mao, Z.-W., Liu, S.-J., Wang, S., Wen, M., Luo, K.-K., Hu, F.-Z., Wu, C., Liu, Q.-F., 2022. Blood cell characterization and transcriptome analysis reveal distinct immune response and host resistance of different ploidy cyprinid fish following *Aeromonas hydrophila* infection. Fish Shellfish Immun. 120, 547–559.

Yang, Y., Chen, F., Chen, H.Y., Peng, H., Hao, H., Wang, K.J., 2020. A novel antimicrobial peptide scyreprocin from mud crab *Scylla paramamosain* showing potent antifungal and anti-biofilm activity. Front. Microbiol. 11, 1589.

Yeaman, M.R., Yount, N.Y.J.P., 2005. Mechanisms of antimicrobial peptide action and resistance - part II. Pharmacol. Rev. 5, 4.

Zasloff, M., 2002. Antimicrobial peptides of multicellular organisms. Nature. 415 (6870), 389–395.

Zhang, W., An, Z., Bai, Y., Zhou, Y., Chen, F., Wang, K.-J., 2023. A novel antimicrobial peptide Scyreptin$_{1\text{-}30}$ from *Scylla paramamosain* exhibiting potential therapy of *Pseudomonas aeruginosa* early infection in a mouse burn wound model. Biochem. Pharmacol. 218, 115917.

Zhou, Q.-J., Wang, J., Mao, Y., Liu, M., Su, Y.-Q., Ke, Q.-Z., Chen, J., Zheng, W.-Q., 2019. Molecular structure, expression and antibacterial characterization of a novel antimicrobial peptide NK-lysin from the large yellow croaker *Larimichthys crocea*. AQUACULTURE. 500, 315–321.

Zhu, X., Chen, F., Li, S., Peng, H., Wang, K.J., 2021. A novel antimicrobial peptide Sparanegtin identified in *Scylla paramamosain* showing antimicrobial activity and immunoprotective role *in vitro* and *vivo*. Int. J. Mol. Sci. 23 (1).